Temperature dependence and short-range electrolytic interactions within the e-PPC-SAFT framework

Juan Sebastián Roa Pinto, Nicolas Ferrando, Jean-Charles De Hemptinne, Amparo Galindo

Temperature dependence and short-range electrolytic interactions within the e-PPC-SAFT framework

Juan Sebastián ROA PINTO, Nicolas FERRANDO, Jean-Charles de HEMPTINNE, Amparo GALINDO

Abstract

Understanding and modelling electrolyte systems is of interest both in an industrial context and from a fundamental point of view. Their importance is related to their key role played in traditional and emerging industries, and to the ubiquitous presence of saline solutions in biological, chemical, and geological environments. The development of electrolyte equations of state has advanced greatly in recent years, with the aim to describe the properties of electrolyte systems using a limited number of parameters, in a way that allows describing accurately the equilibrium properties of these solutions. Here, we explore the temperature and salt concentration dependence of various PPC-SAFT-based models, using simple alkali halide salts (primarily NaCl). The dispersion and association free-energy terms characteristic of SAFT-like equations are compared for the description of the ion-solvent non-Coulombic interactions. Several formulations of the dielectric constant are also investigated. In all models the MSA term is used to account for the electrostatic interactions between the ions and the Born term is added to model the ion-solvent electrostatic interactions. The molecular model parameters are determined by comparison to experimental enthalpy of solution, activity coefficient, osmotic coefficient and apparent molar volume data.
We find that equivalent results can be obtained with or without incorporating a explicit salt concentration dependence in the treatment of the dielectric constant; the most accurate results (smallest average absolute relative deviation) when comparing to experimental the data chosen are found in the case that salt concentration is not explicitly considered. For each approach, the most sensitive parameters are identified, which makes it possible to reduce the number of adjustable parameters without significantly affecting the overall quality of the model. We find that both the approach incorporating a dispersion term and that using an association term in the treatment of short-range interactions yield similar results. Unfortunately, none of the models can describe accurately and with physically meaningful parameters the correct low-temperature trend of the mean ionic activity coefficient observed experimentally.

Keywords: Equation of State, Born, ion pairing, solvation

1 Introduction

Electrolyte solutions are present in traditional industries, such as pharmaceutical, nuclear, and oil and gas, and also in emerging industries in the context of green-energy production, such as in bio-refining, underground gas storage, battery production, water treatment and the metal industry and recycling. Phase equilibrium calculations are a fundamental part of both the piloting and the design of processing plants. For example, in biorefining, the presence of electrolytes causes a significant change in the equilibrium of complex systems, especially in the liquid-liquid equilibrium (LLE). Ions affect the hydrogen-bonding structure as well as other intermolecular forces of the system, such that the mutual solubility between solvents (in mixed-solvent systems) changes in either phase (water-rich and organic-rich). In this context, thermodynamic models capable of delivering accurate properties of such systems are especially important, including models suitable to treat the mutual solubilities of, water and organic solvents in the presence of salts [1]. In underground storage of hydrogen in salt caverns, the prediction of the vapour-liquid equilibrium (VLE) between gas and saturated brines, is necessary to correctly size surface facilities during preliminary design phase, and to determine the storage performance and improve its exploitation during operations [2]. Electrolytes are also often found pharmaceutical processes, in which. thermodynamic models capable of predicting the solubility of active pharmaceutical ingredients in water and organic solvents plays a key role in the discovery and formulation of new drugs in the design, synthesis, extraction, purification, formulation, absorption and distribution in body fluids [3]. The need for efficient and accurate thermodynamic data and models is a common denominator for these industries.

Notwithstanding their industrial and scientific importance, the prediction and calculation of thermodynamic properties of electrolytes and phase equilibrium in the presence of ions with equation-of-state approaches remains a significant challenge. Many reviews of the thermodynamics of electrolyte solutions have been presented in the literature; e.g., Donohue et al. [4] reviewed Pinsky and Takano [5] Maribo-Mogensen [6, 7] and Ahmed [8, 9].

Kontogeorgis et al. [7] have recently reviewed the state of the art on the modelling of electrolyte systems, highlighting open questions in related to this challenge: the formation of ion pairs, the importance of the Born term, the best way to parameterize the models, how the dielectric constant should be modelled, and which model should be used to take into account the electrostatic interactions, are discussed in their review. These questions give an idea of the most important current issues in the study of electrolyte systems. For some of them some consensus exists. For example, Maribo-Mogensen et al. [10] have demonstrated that the most commonly used theories for incorporating the electrostatic interactions between ions (the Debye-Hückel and MSA approaches) are practically equivalent in their ability to provide accurate descriptions of the experimental phase behaviour of electrolyte solutions (subject to the characterisation of the model parameters in each approach). Little consensus exists for some of the other questions however, and multiple points of view can still be found. This is the case of the use and meaning of the Born term: authors [9, 11–14] defend its use stating that it describes ion-solvent interactions in models where the solvent polarity is not accounted for otherwise, and in primitive models [13]. Other authors such as Simonin et al. [15] suggest that this term should not be included in models for electrolytes, as its magnitude greatly overestimates the ion-dipole contribution for most systems. It is important to mention, however, that the correct sign of the solvation energy of ionic species, and the partitioning of ionic species in the liquid phase, cannot be modelled naturally without the inclusion of this free-energy term in models that do not otherwise account for solvent-ion electrostatic interactions.

The model used to incorporate the dielectric constant is also of interest, as its precise value has a direct impact on both the Born and ion-ion (DH or MSA) free-energy terms. The dielectric constant is function of the thermodynamic state, and a such a function of temperature and pressure (or density/volume) as well as concentration of the salt. The model proposed by Schreckenberg [13] is convenient as it depends on temperature and volume, as it should be in an equation of state context, and it implicitly accounts for changes in concentration through the density-dependence of the solvent (i.e., note that concentration

changes result in density changes of the solution). The salt concentration dependence can also be taken into account by either the Pottel [16] or the Simonin models [17].

The formation of ion-pairs is rarely accounted for in equation of state models of strong electrolytes, as complete dissociation of the salt is assumed from the outset. At high temperatures and in non-aqueous solvents however, the formation of ion-pairs can have an important effect on the thermodynamics of the system. Held [18] for example points out that ion pairing does not only occur in systems with low water content or with mixed solvents, but also in aqueous systems, even at moderate salt concentrations. Simonin et al. [19], have developed a model that combines the MSA with ion pair formation (BiMSA). In SAFT frameworks, attractive interactions between ions can be included through dispersion [20–22] (although not strictly pairing) and association [9, 11] terms. These terms are account for attractive interactions between neutral molecules but can be used to mimic the very strong ion-ion or ion-solvent interactions, to a degree. The formation of ion pairs is inversely linked to the solvation of the ions, since the more ions are solvated, the less chance of ion pair formation, and vice versa. For this reason, it is of interest to consider ion-pairing and solvation together.

Furthermore, the quality of a given thermodynamic model highly depends on the experimental data used in its parameterisation. Key experimental properties typically used in the study of electrolyte systems are mean ionic activity coefficient, osmotic coefficient, liquid (single phase or saturate) density, and vapour pressure. Properties such as the enthalpy, and Gibbs-free energy of solution can also be used. The enthalpy is related to the temperature derivative of the Gibbs energy, and as such constitutes a stringent test of the global quality of the model

In the current work, a number of modelling approaches are compared in their ability to reproduce experimental equilibrium properties of aqueous solutions of NaCl. The mean ionic activity coefficient, the osmotic coefficient, the enthalpy of solution and the apparent molar volume are used in the comparison, and especial emphasis is placed in reproducing the temperature dependence of the ionic activity coefficient. As well as carrying out careful parametrisation of the models proposed, an effort is made to keep the number of molecular model parameters to a minimum, and to ensure that their values are physically meaningful. We use on NaCl as the main case study, and extension to other alkali halide is proposed. In section 2, an analysis of the data and the key properties used for modelling electrolytes are presented. In sections 3 and 4 the models proposed are presented together with the different free-energy contributions incorporated, as well as the parameterization strategies that have been used. In sections 5 and 6 a discussion of the results and conclusions is presented.

2 Thermodynamic property data

Mean ionic activity coefficient (MIAC), osmotic coefficient, apparent molar volume, and enthalpy of solution data are considered. The MIAC directly relates to the excess chemical potential of the ionic species, while the osmotic coefficient is closely related to the vapour pressure and chemical potential of the solvent. These two properties are related by the Gibbs-Duhem relation [14, 23], some authors use both in model development [24], while others use only one to determine parameters and the other one to assess the validity of the models develop [14]. The apparent molar volume provides a stringent test related to the size parameters (ion and solvent diameters) in the models, while the enthalpy of solution is chosen to capture the temperature dependent behaviour of the infinite dilution regime. We chose not to compare to the Gibbs-free energy of solvation because this property is used to fix Born diameters. As will be shown later in section 5.2 the Gibbs energy of solvation depends strongly on the Born term.

At a specified temperature and total volume, we consider fluid mixtures consisting of water (the solvent (A)) and a salt (the solute) which is fully dissociated into its constituent ions following an equilibrium reaction. For a salt $X_{\nu_+}Y_{\nu_-}$, the equilibrium can be described as:

$$X_{\nu_+}Y_{\nu_-} \rightleftarrows \nu_+ \cdot X^{Z_+} + \nu_- \cdot Y^{Z_-} \tag{1}$$

where ν_+ and ν_- are the stoichiometric coefficients of the cation (X) with valency $\boldsymbol{Z}_+$ and the anion (Y) with valency $\boldsymbol{Z}_-$, respectively. In our case we consider only monovalent salts $\nu_+ = \nu_- = 1$, and the salt is further written as XY.

Molarity is often the unit of concentration used in electrolytic systems. Molality is defined as the number of moles of a given salt (XY) per kilogram of solvent (A). However, in calculations with equations of state it is the mole fraction that is used. The mole fraction of a given ion i can be calculated from the molality as:

$$x_i = \frac{\nu_i m_{XY}}{\nu \cdot m_{XY} + 1/MW_A} \tag{2}$$

where ν_i is the stoichiometric coefficient of ion i, $\nu = \sum_{i=1}^{n_{ions}} \nu_i$, and MW_A denotes the molecular weight of the solvent in units of kg mol^{-1}.

2.1 Mean ionic activity coefficient

The activity coefficient describes the deviation of the fugacity with respect to an ideal solution behaviour [25]:

$$f_i = x_i \cdot f_i^* \cdot \gamma_i \tag{3}$$

In this equation, f_i stands for the fugacity of the ion i, x_i is the mole fraction of the ion i, and f_i^* is the fugacity in the reference state. Activity coefficients are often determined by carrying out electromotive force (EMF) measurements, on cells in which the concentration of the ion of interest is known [26]. In addition, despite some attempts to do so [27, 28], it is very difficult to distinguish between cation and anion activity coefficient, as both are simultaneously present in the solution. The mean ionic activity coefficient which is defined on a molality basis (indicated by a superscript m) is defined as:

$$\gamma_{\pm}^m = \left(\gamma_X^{\nu_+,m} \cdot \gamma_Y^{\nu_-,m}\right)^{\frac{1}{\nu_+ + \nu_-}} \tag{4}$$

where $\gamma_{\pm}^m$ is the mean ionic activity coefficient and $\gamma_{\mathrm{X}}^{\boldsymbol{\nu}_+,\mathrm{m}}$, $\gamma_{\mathrm{Y}}^{\boldsymbol{\nu}_-,\mathrm{m}}$ are the activity coefficients of the cation and anion, respectively. When molality is used as concentration unit, the molality-based activity coefficient is thus defined. Yet, the equation of state framework is based on mole fractions, and the mole fraction-based activity coefficient of an ion i (γ_i) is obtained from the fugacity coefficients as follows:

$$\gamma_i = \frac{\varphi_i}{\varphi_i^*} \tag{5}$$

where, φ_i is the fugacity coefficient of ion i in the fluid mixture and φ_i^* its fugacity coefficient in the reference state (pure water). The mole fraction-based activity coefficient is converted into molality-based activity coefficient (${\gamma_i}^m$) using:

$${\gamma_i}^m = \gamma_i \cdot x_A \tag{6}$$

where x_A is the mole fraction of the solvent.

The trend of the mean ionic activity coefficient with composition and temperature has recently been discussed by Vaque et al. [29]. At fixed temperature, the MIAC initially decreases as the concentration of ions in solution increases; authors [29, 30] attribute this decrease to dominating electrostatic forces, and higher concentrations, related to what is called 'solvation' (Figure 1). This increase may be more or less pronounced depending on temperature and salt considered.

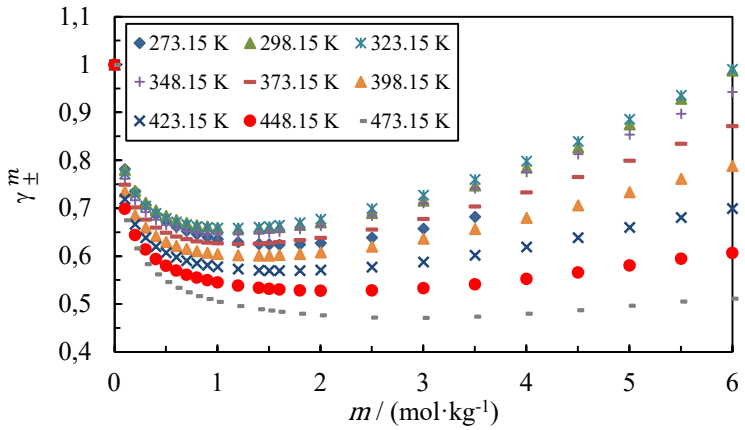

Figure 1 : Experimental mean ionic activity coefficient data for NaCl at different temperatures [31, 32]. The corresponding pressure is 1 atm for the data at temperatures between 273.15 and 373.15 K, while saturation pressure was used in the measurements at higher temperatures.

2.2 Osmotic coefficient

The osmotic coefficient (ϕ) is a measure of the deviation of the solvent from the ideal behaviour[33]:

$$\phi = \frac{-\ln a_A}{M_A \cdot (\nu_+ + \nu_-) \cdot m_{XY}} = -\ln\left(x_A\ \gamma_A\right)\frac{x_A}{1 - x_A} \tag{7}$$

where a_A is the activity of the solvent (A), M_A is the molecular weight of the solvent, m_{XY} is the molality of the salt (XY) and γ_A is the activity coefficient of the solvent.

Osmotic coefficient can be measured using various methods such as freezing point depression, boiling point elevation and the isopiestic method [26]. It can be calculated from either the difference between the measured freezing point and that expected for an ideal solution, or from differences in boiling temperatures [26]. In the isopiestic method [34] the solvent activity of a sample is determined by placing the sample in equilibrium with a reference solute of known solvent activity. After several days or weeks (when equilibrium is reached between the two samples), the masses of the samples are measured to determine the amount of water in each. The solvent activity of the reference salt solution is a known function of the salt concentration. At equilibrium, the water activities in both samples will be equal, therefore, the water activity of the salt solution under study will be known.

As mentioned above, it is important to note also that the osmotic coefficient is directly related to the molality-based activity coefficient through the Gibbs–Duhem relation [23]; i.e.:

$$\phi = 1 + \frac{1}{m_{XY}} \int_0^{m_{XY}} m \frac{\partial ln(\gamma_{\pm}^{m})}{\partial m_{XY}} dm_{XY} \quad (8)$$

2.3 Apparent molar volume

The apparent molar volume is defined as [26]:

$$v_{\pm} = \frac{(v - x_A v_A)}{(x_+ + x_-)} \quad (9)$$

where v and v_A are the molar volumes of the solution and of the solvent respectively, and x_+ and x_- are the mole fractions of the cation and the anion.

While the molar density of an electrolyte decreases with salinity, the molar volume and the apparent molar volume goes up (see Figure 2). In practice, it is impossible to differentiate the contribution of separate ions, and hence a representation of ± is used to denote the overall apparent molar volume for the solution. This property expresses the change in the volume of the solution when a salt is added. As can be seen in Figure 2 the change in this property with mole fraction is larger than for the molar volume of the solution, making it more sensitive to the values of parameters in the model.

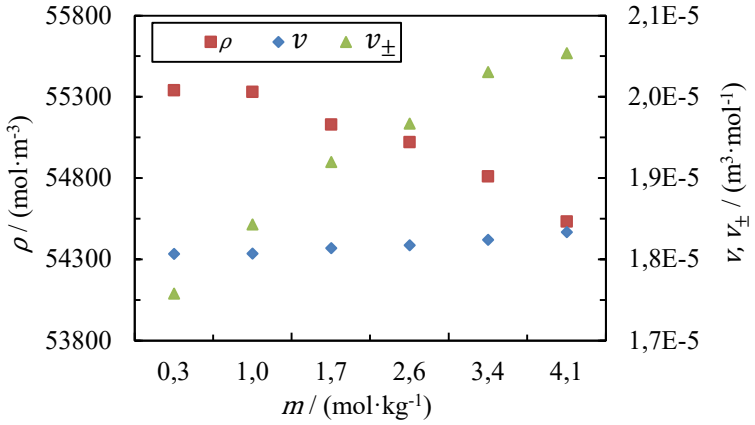

Figure 2 : Molar density ρ, molar volume v and apparent molar volume $v_{\pm}$ as a function of NaCl concentration at 298 K [35, 36].

2.4 The enthalpy of solution

The molar enthalpy of solution refers to the change of enthalpy when a certain quantity of solute is mixed with the solvent. Experimentally it is obtained by slowly adding a salt to the solution (that is initially pure), and measuring the heat required to maintain a constant temperature with a calorimeter. The molar enthalpy of solution (h^{sol}) may be expressed as:

$$h^{sol} = \frac{H - (n_A h_A^* + n_{XY} h_{XY}^{*,S})}{n_{XY}} \quad (10)$$

where the total enthalpy of the solution, H, is written as the sum of number of moles times the partial molar enthalpies ($\bar{h}_i$) of the compounds [29]:

$$H = n_A \bar{h}_A + n_{XY} \bar{h}_{XY} = n_A (h_A^* + \bar{h}_A^E) + n_{XY} (h_{XY}^{\infty} + \bar{h}_{XY}^{E'}) \quad (11)$$

Here, h_A^* is the molar enthalpy of pure solvent A (which is the reference state enthalpy of the solvent), $\bar{h}_A^E$ is the excess partial molar enthalpy of the solvent A, h_{XY}^{∞} is the molar enthalpy of solute (salt XY) at infinite dilution (which is the reference state enthalpy of the solute), $\bar{h}_{XY}^{E'}$ is the excess partial molar enthalpy of solute in the asymmetric convention. In equation (12), the enthalpy difference is divided by the amount (number of moles) of salt added. Hence:

$$\boldsymbol{h^{sol}} = \frac{\boldsymbol{n_A \bar{h}_A^E + n_{XY}\left(h_{XY}^{\infty} - h_{XY}^{*,S} + \bar{h}_{XY}^{E'}\right)}}{\boldsymbol{n_{XY}}} = \frac{\boldsymbol{n_A \bar{h}_A^E + n_{XY}\bar{h}_{XY}^{E'}}}{\boldsymbol{n_{XY}}} + \left(\boldsymbol{h_{XY}^{\infty} - h_{XY}^{*,S}}\right)$$
$$= \frac{(n_A + n_{XY}) * h^{M'}}{n_{XY}} + \left(h_{XY}^{\infty} - h_{XY}^{*,S}\right) = \frac{h^{M'}}{x_{XY}} + \left(h_{XY}^{\infty} - h_{XY}^{*,S}\right) \quad (12)$$

where the prime (') refers to the asymmetric convention. The asymmetric mixing enthalpy is written as:

$$h^{M'} = x_A \bar{h}_A^E + x_B \bar{h}_B^{E'} \quad (13)$$

The partial molar excess enthalpy can be obtained from the activity coefficient as:

$$\bar{h}_A^E = \bar{h}_A - h_A^* = -RT^2 \left.\frac{\partial ln\, \gamma_A}{\partial T}\right|_N \quad (14)$$

In the case that an asymmetric activity coefficient is used (electrolyte systems), the excess partial molar enthalpy ($\bar{h}_{XY}^{E'}$) can be calculated as:

$$\bar{h}_{XY}^{E'} = \bar{h}_{XY} - h_{XY}^{\infty} = -RT^2 \left.\frac{\partial ln\, \gamma_{XY}{}'}{\partial T}\right|_N \quad (15)$$

and hence

$$\frac{h^{M'}}{RT^2} = -\left(x_A \left.\frac{\partial ln\, \gamma_A}{\partial T}\right|_N + x_{XY} \left.\frac{\partial ln\, \gamma_{XY}{}'}{\partial T}\right|_N\right) \quad (16)$$

Furthermore, most of the data available correspond to highly dilute solutions ($x_A \approx 1$ and therefore $\gamma_A \approx 1$). Therefore, combining equations (12) and (16), one finds:

$$h^{sol} \approx -RT^2 \left.\frac{\partial ln\, \gamma_{XY}{}'}{\partial T}\right|_N + \left(h_{XY}^{\infty} - h_{XY}^{*,S}\right) \quad (17)$$

In order to transform the enthalpy of solution in terms of the mean ionic activity coefficient $\left(\gamma_{\pm}^{m}\right)$ it is necessary to use equation (6), and to use the equivalence between the activity of the salt and that of the ions (i.e., $m_{XY}\, \gamma_{XY}^{m} = m_X \gamma_X^{m} \cdot m_Y \gamma_Y^{m}$ for a 1:1 salt) [37], which yields $\gamma_{XY}{}' = \frac{m_{XY}}{x_A}\left(\gamma_{\pm}^{m}\right)$. The enthalpy of solution is thus obtained as:

$$h^{sol} \approx -2RT^2 \frac{m_{XY}}{x_A} \left.\frac{\partial ln \gamma_{\pm}^{m}}{\partial T}\right|_N + \left(h_{XY}^{\infty} - h_{XY}^{*,S}\right) \quad (18)$$

or, in other words, the enthalpy of solution is the result of a sum of a constant term $\left(h_{XY}^{\infty} - h_{XY}^{*,S}\right)$ and a term related to the change in the MIAC with temperature ($\left.\frac{\partial ln \gamma_{\pm}^{m}}{\partial T}\right|_N$).

In Figure 3 the enthalpy of solution [38] as a function of salinity is shown. It can be seen that it is not zero in the limit of pure solvent:

$$\lim_{x_{XY}\to 0}\left(h^{sol}\right) = \lim_{x_{XY}\to 0}\left(\frac{h^{M'}}{x_{XY}}\right) + \left(h_{XY}^{\infty} - h_{XY}^{*,S}\right) \quad (19)$$

In addition, this limit is not equal to the heat of solution $\left(h_{XY}^{\infty} - h_{XY}^{*,S}\right)$, because $\lim_{x_{XY}\to 0}\left(\frac{h^{M'}}{x_{XY}}\right) \neq 0$.

As suggested by Vaque Aura [29], an interpolation of the enthalpies at infinite dilution as a function of temperature was proposed:

$$\lim_{x_{XY}\to 0}\left(h^{sol}\right) = aT^2 + bT + c \qquad (20)$$

where a, b and c are empirical parameters.

A linear behaviour was found for the salts KCl, NaBr and KBr. For NaCl a quadratic behaviour is reported [29]. In Table 1 the parameters used for equation 20, for the 4 salts used in this work are reported.

Table 1 : Parameters used for the calculation of the enthalpy of solution at infinite dilution, for NaCl, KCl, NaBr and KBr. *a*, *b* and *c* are the parameters used in the equation (20).

Salt	***a***	***b***	***c***	references
NaCl	2.3343	-1502.8	244509	[38, 39]
KCl	0	-143.32	60220	[39, 40]
NaBr	0	-120.46	35422	[41, 42]
KBr	0	-170.40	71112	[43]

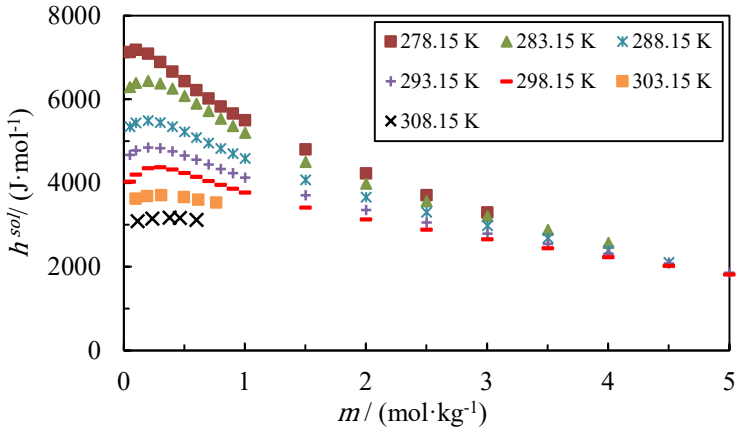

Figure 3 : Experimental molar enthalpy of solution of aqueous NaCl [38] at different temperatures and 1 bar pressure.

Thus, when the enthalpy of solution decreases with composition, as observed in the largest part of the composition range (see Figure 3), the slope of the activity coefficient with temperature $\left(\frac{\partial ln\gamma_{\pm}^{m}}{\partial T}\Big|_{N}\right)$ is expected to increase.

In Figure 4 the natural logarithm of the mean ionic activity coefficient as a function of temperature is shown for two salt concentrations. As can be seen, in the lower temperature range (below 308 K), the slope is slightly more positive in the case of 3 molal concentration than in the 1 molal case. This behavior is directly related to the behavior of the enthalpy of solution. The larger the slope (which is equal to the derivative of *ln*(MIAC) with respect to temperature) the lower the value of the enthalpy of solution. This shows that there is a correlation between these two properties.

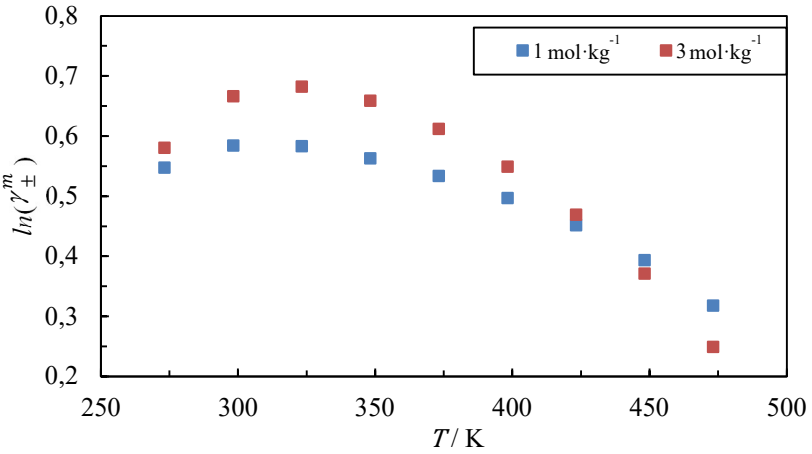

Figure 4 : Variation of the natural logarithm of experimental mean ionic activity coefficient ($\ln(\gamma_{\pm}^{m})$) with temperature at fixed molality.

Few authors use the enthalpy of solution in model development and assessment, as capturing the temperature change of the MIAC of strong electrolytes is an especially stringent test of any model.

3 Modelling framework

In the PPC-SAFT EoS [11, 44], the residual Helmholtz free energy of the electrolyte mixture is given as a sum of terms as:

$$A^{Res} = A^{HS} + A^{Disp} + A^{Chain} + A^{Polar} + A^{Assoc} + A^{MSA} + A^{Born} \quad (21)$$

accounting for of hard sphere (A^{HS}) repulsion interactions, van der Waals interactions (also known as dispersion interactions A^{Disp}), a term accounting for the formation of chains (A^{Chain}) in non-spherical models, polar (A^{Polar}) and association interactions, (A^{Assoc}) together with long-range ion-ion interactions and solvent-ion interactions. The theory of Debye-Hückel [45] or of Blum (primitive Mean spherical approximation) [46], have been shown to be almost equivalent by Maribo-Mogensen et al [10] in terms of their accuracy in the treatment of the Coulombic contribution for experimental electrolytes. In the current study, the primitive MSA is used (A^{MSA}). Ion-solvent interactions (also called solvation interactions) are included. In our current work the classic term developed by Born [47] is used.

It is our intention to evaluate and discuss several options in the choice of the terms in the PPC-SAFT EoS. In Table 2 the combinations studied in our current work are shown. The proposed models are divided into two groups: The first group (models of type 1) contains models that use the dispersion term to describe the short-range interactions involving ions. The second group (models type 2) contains models that use the association term to model the short-range interactions between ions. All other terms are identical. The distinction is implemented through a priory assumptions on the values of the model parameters. In type 1 models, ion-ion association energies are set to zero, while in models of type 2, the ion-ion dispersive energies are set to zero. A further subdivision is made based on the way the dielectric constant is used. Three models for the calculation of the dielectric constant are considered. They are further discussed in section 3.7.

Table 2 : PPC-SAFT EoS models for compared in the current work [a].

Interaction	Model					
	Dispersive models (Models 1)			Associative models (Models 2)		
	1.0	1.1	1.2	2.0	2.1	2.2
Hard sphere	all molecules	all molecules	all molecules	all molecules	all molecules	all molecules
Dispersion	solv-solv ion-solv ion-ion	solv-solv ion-solv ion-ion	solv-solv ion-solv ion-ion	solv-solv	solv-solv	solv-solv
Association	solv-solv	solv-solv	solv-solv	solv-solv ion-solv cat-ani	solv-solv ion-solv cat-ani	solv-solv ion-solv cat-ani
Polar	solv-solv	solv-solv	solv-solv	solv-solv	solv-solv	solv-solv
Born	ion-solv	ion-solv	ion-solv	ion-solv	ion-solv	ion-solv
MSA	cat-ani	cat-ani	cat-ani	cat-ani	cat-ani	cat-ani
Dielectric constant	Schreckenberg	Pottel	Simonin	Schreckenberg	Pottel	Simonin

[a]. The meaning of the abbreviations presented in the table are: solv-solv = solvent-solvent, ion-solv = ion-solvent, ion-ion = all the ion-ion interactions and cat-ani = cation-anion interactions. In the current work the solvent is always water.

Table 3 : Pure component parameters of water used in the current work, taken from [9]. m is the chain length, σ_w^{HS} is the hard sphere diameter, ε_w is the dispersion energy, ε_w^{AB} is the association energy, κ_w^{AB} is the association volume, M is the association sites, μ is the dipole moment and x_p is the dipole fraction.

Parameter	Value	Parameter	Value
$\boldsymbol{\sigma_w^{HS}}$ /Å	See Note	ε_w^{AB}/k_B /K	1813
$\boldsymbol{m_w}$	1.02122	κ_w^{AB}	0.044394
$\boldsymbol{\varepsilon_w/k_B/K}$	201.747	M	4
$\boldsymbol{\mu}$ /D	1.85	x_p	0.276

Note: A temperature-dependent diameter is used only for water molecules in this study. The segment diameter of pure water is given by [48] (in Å): $\sigma_w^{HS} = 2.2423 + 0.51212\exp(0.001126 \cdot T) + \frac{9904.13}{T^2}$, with T the temperature in K. With these parameters the mean absolute deviation for density is 0.72% and for vapour pressure is 2.32% [9].

3.1 Hard sphere term

In the hard sphere term the repulsive interactions of the molecules within the system are accounted for. The equation used to calculate the contribution of repulsive interactions to Helmholtz energy is given as [49, 50]:

$$\frac{A^{HS}}{RT} = \frac{6V}{\pi N_{Av}}\left[\left(\frac{\zeta_2^3}{\zeta_3^2} - \zeta_0\right) ln(1-\zeta_3) + \frac{3\zeta_1\zeta_2}{1-\zeta_3} + \frac{\zeta_2^3}{\zeta_3(1-\zeta_3)^2}\right] \tag{22}$$

with:

$$\xi_k = \frac{\pi N_A \rho}{6}\sum_{i=1}^{n} x_i\left(d_i(T)\right)^k \quad \text{and} \quad d_i(T) = \sigma_i^{HS}\left[1 - \lambda_i e^{\left(-3\frac{\varepsilon_i}{RT}\right)}\right] \tag{23}$$

where, ρ is the molar density of the fluid, σ_i^{HS} is the hard sphere diameter, ε_i is the dispersive energy parameter, λ_i is the softness parameter which is equal to 0.12 (except for water in the model used in this work: λ_i= 0.203). For water, the temperature dependence of $d_i(T)$ was modified by Ahmed et al. [9]. N_A is Avogadro's number, $d_i(T)$ is the segment diameter proposed in [51], x_i is the mole fraction of the component i, V is the volume and R is the universal gas constant. The hard sphere term is characterised by the hard sphere diameter (σ_i^{HS}), which is specific for each ion.

3.2 Dispersion term

The Helmholtz energy for dispersion is given as [8]:

$$\frac{A^{Disp}}{RT} = \frac{A_1}{RT} + \frac{A_2}{RT} \tag{24}$$

where:

$$\frac{A_1}{RT} = -2\pi\rho\,\overline{\varepsilon\sigma^3}\int_1^{\infty} g_{ij}^{hs}(x_i,\rho)x^2dx \tag{25a}$$

$$\frac{A_2}{RT} = -\pi\rho\left(Z^{hs} + \rho\frac{\partial Z^{hs}}{\partial\rho}\right)^{-1}\overline{\varepsilon^2\sigma^3}\,\frac{\partial}{\partial\rho}\left[\rho\int_1^{\infty} g_{ij}^{hs}(x_i,\rho)x^2dx\right] \tag{25b}$$

$$g_{ij}^{HS} = \frac{1}{1-\xi_3} + 3\frac{d_{ij}\xi_2}{\left(1-\xi_3\right)^2} + 2\frac{\left(d_{ij}\xi_2\right)^2}{\left(1-\xi_3\right)^3} \tag{26}$$

where $x = \frac{r}{\sigma}$ is the reduced radial distance from the centre of a segment, Z^{hc} is the compressibility factor, $g_{\mathrm{ij}}^{\mathrm{HS}}$ is the radial distribution function that expresses the probability of finding a molecule j at a distance d_{ij} from molecule i [25, 50, 52] and ξ_k is calculated by equation (23), $\overline{\varepsilon\sigma^3}$ and $\overline{\varepsilon^2\sigma^3}$ represent average values obtained by a mixing rule based on the Van der Waals one fluid theory [52]:

$$\overline{\varepsilon\sigma^3} = \sum_i^n \sum_j^n x_i\, x_j \left(\frac{\varepsilon_{ij}}{kT}\right) \left(\sigma_{ij}^{HS}\right)^3 \tag{27}$$

$$\overline{\varepsilon^2\sigma^3} = \sum_i^n \sum_j^n x_i\, x_j \left(\frac{\varepsilon_{ij}}{kT}\right)^2 \left(\sigma_{ij}^{HS}\right)^3 \tag{28}$$

The dispersion term requires two parameters: the distance of closest approach (σ_{ij}^{HS}) and the binary dispersion energy (ε_{ij}). The distance of closest approach is computed directly from the hard sphere diameters:

$$\sigma_{ij}^{HS} = \frac{\sigma_i^{HS} + \sigma_j^{HS}}{2} \tag{29}$$

In the present study the binary dispersion energy is presented directly. In dispersive models (models 1), six such interactions will be considered: water-water (the parameters are taken directly from Table 3), anion-water, cation-water, cation-anion as well as anion-anion and cation-cation. In associative models (models 2), only water-water dispersion energy is considered.

3.3 Association term

The Wertheim association term considers the short-range directional interactions. It can be considered as a pseudo-chemical term that describes the formation of a chemical bond between sites. Hence, the first step when using this term is to define the number of sites and their charge, for each species. The association term contribution to the Helmholtz energy is given as [53]:

$$\frac{A^{Assoc}}{RT} = \sum_i n_i \sum_{A_i} \left[\left(lnX^{A_i} - \frac{X^{A_i}}{2}\right) + \frac{1}{2}M_i\right] \tag{30}$$

where M_i is the number of association sites in a molecule i and X^{Ai} is the fraction of molecules of type i not bonded at site A computed as:

$$X^{A_i} = \left[1 + N_{Av} \sum_{B_j} \left(\rho X^{B_j} \Delta^{A_i B_j}\right)\right]^{-1} \tag{31}$$

The equilibrium constant is expressed as $\Delta^{A_i B_j}$ between the A site of molecule i and the B site of molecule j. The equation used to calculate the this constant is [77]:

$$\Delta^{A_i B_j} = d_{ij}^3 g_{ij}^{HS} k^{A_i B_j} \left[exp\left(\frac{\varepsilon^{A_i B_j}}{kT}\right) - 1\right] \quad \text{with} \quad d_{ij} = \frac{\sigma_i^{HS}\sigma_j^{HS}}{\sigma_i^{HS}+\sigma_j^{HS}} \tag{32}$$

where g_{ij}^{HS} is the radial distribution function and given in equation 26.

The site-site association interactions ($\Delta^{A_i B_j}$) are characterized by two binary parameters, the association energy ($\varepsilon^{A_i B_j}$) and the association volume ($k^{A_i B_j}$). In dispersive models, only water has interaction sites (4C type as shown in Table 3). On the other hand, in associative models (models 2) association interactions are used for ion-ion interactions too. We follow the work of Ahmed et al. [8], and describe the cations using 7 interaction sites and the anions with 6 sites.

3.4 Polar term

An improved representation of the behaviour of water can be obtained by taking into account the polarity of the molecule [48, 54, 55]. Here we use the term proposed by Jog and Chapman [56] to describe this type of interactions:

$$\frac{A^{polar}}{RT} = \frac{A_2^{polar}}{1 - \frac{A_3^{polar}}{A_2^{polar}}} \tag{33}$$

$$A_2^{polar} = -\frac{2\pi\rho}{9(kT)^2}\sum_i^n\sum_i^n x_i\, x_j m_i m_j x_{pi} x_{pj} \frac{\mu_i^2\mu_j^2}{d_{ij}^3} I_{2,ij} \tag{34}$$

$$A_3^{polar} = -\frac{15\pi^2\rho^2}{9(kT)^3}\sum_i^n\sum_j^n\sum_k^n x_i\, x_j x_k m_i m_j m_k x_{pi} x_{pj} x_{pk} \frac{\mu_i^2\mu_j^2\mu_k^2}{d_{ij}d_{jk}d_{ik}} I_{3,ijk} \tag{35}$$

Here μ_i is the dipole moment and x_{pi} the fraction of the polar hard spheres of molecule i. $I_{2,ij}$ and $I_{3,ijk}$ are correlations representing integrals over statistical properties.

3.5 Mean spherical approximation

The primitive mean spherical approximation (MSA) describes long-range cation-anion interactions (coulombic interactions). The unrestricted of MSA is used in this work, in which each ion has a specific MSA diameter (σ_i^{MSA}) different than the hard-sphere diameter The final expression of the Helmholtz energy is given as [46]:

$$\frac{A^{MSA}}{RT} = -\frac{N_A e^2}{4\pi\,\varepsilon_o\varepsilon_r RT}\sum_i^{ions}\frac{n_i {Z_i}^2 \Gamma}{1+\Gamma\sigma_i^{MSA}} + \frac{V\Gamma^3}{3\pi}kT \tag{36}$$

where ε_r is the dielectric constant of the fluid (see section 3.7), ε_o is the dielectric constant in the vacuum (8.85418x10^{-12} C mol^{-1}), n_i is the number of moles of ion i, e is the electron charge (1.60218x10^{-19} C), Z_i is the ion valency, and Γ the shielding parameter that is calculated as follows:

$$4\Gamma^2 = \frac{N_A e^2}{\varepsilon_o\varepsilon_r RT}\sum_i^{ions}\frac{n_i}{V}\left(\frac{{Z_i}^2}{1+\Gamma\sigma_i^{MSA}}\right) \tag{37}$$

3.6 Born term

The Born contribution describes the change in free energy of the ions due to a change in dielectric constant. It was first introduced by Born [47], and now very often used in electrolyte models [9, 11, 57]. It is given by as:

$$\frac{A^{Born}}{RT} = \frac{N_A e^2}{4\pi\,\varepsilon_o RT}\left(1-\frac{1}{\varepsilon_r}\right)\sum_i^{ions}\frac{n_i {Z_i}^2}{\sigma_i^{Born}} \tag{38}$$

where σ_i^{Born} is the Born (solvated) diameter for each ion.

In this work, we have set the value for each ion to the value corresponding to the experimental Gibbs energy of solvation, as suggested by Fawcett *et al.* [58]. Equation (39), is used and the resulting Born diameters are shown in Table 4.

$$\Delta_s G_i = -\frac{N_A Z_i^2 e^2}{4\pi\varepsilon_o\sigma_i^{Born}}\left(1-\frac{1}{\varepsilon_{solvent}}\right) \tag{39}$$

Table 4 : Experimental Gibbs energy of Solvation [58] and Born diameters for each ion. $\Delta_s G_i$ is the Gibbs energy of solvation and σ_i^{Born} is the Born diameter.

Cation	$\Delta_s G_i$ /kJ / mol	σ_i^{Born} / Å	Anion	$\Delta_s G_i$ /kJ / mol	σ_i^{Born} / Å

	[58]			[58]	
Na^+	-424	3.23	Cl^-	-304	4.51
K^+	-352	3.89	Br^-	-278	4.93

3.7 Dielectric constants

When using a primitive model, an empirical correlation for the dielectric constant is required. Maribo-Mogensen [6] reported in his review of electrolytic models, that the majority of studies ignore the volumetric dependence of the dielectric constant (using a correlation of the static permittivity of water as a function of temperature at the saturation line), and the compositional dependence (unless the model is applied to mixed solvents). There are some exceptions [11, 59, 60], in which the authors have used empirical correlations that are function of water density. Inchekel [60] made a comparison of how well NaCl activity coefficients can be matched using two empirical models for the dielectric constant. On the other hand, Ahmed et al. [9] showed that the mean ionic activity coefficient calculations are improved when using the correlation proposed by Schreckenberg [13] for pure compounds (solvent), and adding the Pottel model [16] to take into account the effect of ion species concentration within the system.

Industrial electrolyte models consider usually that the dielectric constant is independent of the ionic concentration, which is not true in practice. Their argument is that the models used to make these calculations (MSA, Debye-Hückel and Born) are developed at infinite dilution conditions [61]. These models provide a corrective energy related to the charging of one ion or the ion-ion interactions. However, considering a thermodynamic cycle explained by Rozmus [62], the composition, temperature, and volume are constant throughout the cycle. The only thing that varies are the interactions between the different species of the system. This means that when considering the interactions involving the ions, the composition of the system is not at infinite dilution, but at the true concentration of the system. This is why a number of authors [9, 11, 60] suggest using a salt concentration-dependent dielectric constant. Maribo-Mogensen [6, 63, 64] has shown that the use of such dependency provides a non-negligible change on the behaviour of the compositional derivative of the Helmholtz energy.

Three models for the dielectric constant are considered in this work: the model of Schreckenberg et al. [13], which describes the property as a function temperature and of the solvent density, in addition to two other models based on the Schreckenberg et al. model but explicit accounting for salt concentration.

Schreckenberg's Model

The correlation proposed by Schreckenberg et al. [13] for the calculation of the dielectric constant is:

$$\varepsilon_r = \varepsilon_{r,Solvent} = 1 + \frac{n_{solvent}}{V} d_v \left(\frac{d_T}{T} - 1\right) \tag{40}$$

where $n_{solvent}$ is the number of moles of solvent V is the volume of system, T is the temperature, d_v and d_T are constants with a value for water of 0.3777 dm^3/mol and 1403 K respectively. Although this model does not consider explicitly the effect of the presence of salts in the solution, there is an implicit dependence through the use of $\frac{n_{solvent}}{V}$.

Pottel's model

This model of Pottel [16] is one of the most widely used to evaluate salt concentration effect on dielectric constant of electrolyte solutions. It is derived from the Onsager equations, linking the dielectric constant of the solution to the ionic compactness of the saturated solution which represents the cavities surrounding each ion [16] , as:

$$\varepsilon_r - 1 = \left(\varepsilon_{r,Solvent} - 1\right) \frac{1 - \xi_3''}{1 + \frac{\xi_3''}{2}} \tag{41}$$

The ion concentration intervenes through the theoretical compactness of the ions (ξ_3''):

$$\xi_3'' = \frac{N_{AV}\pi}{6}\sum_i^{ions}\frac{n_i\left(\sigma_i^{HS}\right)^3}{V} \tag{42}$$

where $\varepsilon_{r,Solvent}$ is the dielectric constant of the solvent (for which the model of Schreckenberg is used), σ_i^{HS} is the hard sphere diameter and V is the volume of the system. This model is purely predictive, as it does not require any additional empirical parameter.

Simonin's model

Simonin's model [17] has a more empirical structure and uses an adjustable parameter α_{ion} (one per ion pair). Thanks to this adjustable parameter, the concentration dependence of the dielectric constant can be better considered.

$$\varepsilon_r = \frac{\varepsilon_{r,Solvent}}{1+\sum_i^{ions}(\alpha_{ion}\,x_i)} \tag{43}$$

where $\varepsilon_{r,Solvent}$ is the dielectric constant of the solvent (computed using the Schreckenberg model, equation (40)), α_{ion} is the adjustable parameter and x_i is the molar fraction of the ions. Roa et al. [2] report that the variation of the parameter (α_{ion}) with respect to the temperature follows a linear trend for the aqueous NaCl solution. Based on this observation, Roa proposed to include two new parameters within Simonin's model. For this, the parameter (α_{ion}) was transformed into.

$$\alpha_{ion}(T) = \alpha_{T,ion}(T-298.15)+\alpha_{o,ion} \tag{44}$$

Therefore, equation (44) can be rewritten as:

$$\varepsilon_r = \frac{\varepsilon_{r,Solvent}}{1+\sum_i^{ions}\left(\left(\alpha_{T,ion}(T-298.15)+\alpha_{o,ion}\right)x_i\right)} \tag{45}$$

where $\alpha_{T,ion}$ and $\alpha_{o,ion}$ are adjustable parameters.

4 Model parameterization for NaCl

In order to analyse the behaviour of the different models proposed, several properties have been selected and tested on a single salt. The objective is to investigate the ability of the models proposed to reproduce different properties, rather than to construct a readily useable model.

The objective function (OF) used is given as:

$$OF = \frac{1}{2}\sum_{j=1}^{n_{ser}} W_s^j \sum_{i=1}^{Npt^j} w_j^i \left(D_{calc}^{i,j} - D_{exp}^{i,j}\right)^2 \tag{46}$$

where n_{ser} is the number of data series, Npt^j is the number of values for the data series j, W_s^j is global weight for each data series j, w_j^i is the local weight for the i^{th} value of data series j, $D_{calc}^{i,j}$ are the calculated data and $D_{exp}^{i,j}$ the experimental data. In practice, the experimental uncertainties may be considered proportional to the experimental value, yielding

$$w_j^i = \left(\frac{1}{err(\%) * D_{calc}^{i,j}}\right)^2 \tag{47a}$$

In some cases, the uncertainty is given in absolute terms:

$$w_j^i = \left(\frac{1}{e^j}\right)^2 \tag{47b}$$

The global weight of the property may be taken as inversely proportional to the number of points, which is why we have:

$$W_s^j = \left(\frac{w_s^j}{Npt_j}\right)^2 \tag{48}$$

where w_s^j should be adapted to the relative importance of the property in the objective function. For each property j.

4.1 Database

A selection among the large amount of data was made according to the internal consistency analysis procedure of Vaque et al. [16]. In Table 5 temperature and concentration ranges used and corresponding references for aqueous NaCl are given.

Table 5 : Number of experimental data points (Npt^j), uncertainty ($err(\%)$ or e^j), data serial weight (w_s^j), temperature and concentration range of each properties used for the optimizations of aqueous NaCl. $\gamma_{\pm}^m$ is the mean ionic activity coefficient, ϕ is the osmotic coefficient, h^{sol} is the enthalpy of solution and $v_{\pm}$ is the apparent molar volume.

	$\gamma_{\pm}^m$	ϕ	h^{sol}	$v_{\pm}$	Reference
Npt^j	220	115	106	73	[31, 32, 35, 38, 65–68]
$err(\%)$ or e^j	2%	5%	50 J/mol	10%	
w_s^j	1	1	0.01	1	
Temperature range / K	273.15-473.15	298.15-573.15	278.15-308.15	278.15-318.15	
Molality range (mol.kg^{-1})	0 - 6	0 - 10	0 - 5	0 - 6	

The four properties described in section 2 are used for model parameterization (mean ionic activity coefficient, osmotic coefficient, apparent molar volume, and enthalpy of solution). These properties vary

in different ways with temperature and salt concentration, making the optimizations challenging. The uncertainties and the weight factors ($err(\%)$ - e^j and w_s^j) used in this work are presented in Table 5. They are selected as follows: the individual uncertainties, $err(\%)$ or e^j are determined based on knowledge from the experimental uncertainties [29]. The weight on each series is estimated in such a way that all four of properties carry a similar weight in the optimal value of the objective function. In Table 6 an example of the contribution of each sub-function to the total objective function is given, based on the data of Table 5.

Table 6 : Contribution of the different sub-objective functions (sOF) to the total objective function (OF) in the regression of the NaCl aqueous solution using model 1.2. $\gamma_{\pm}^{m}$ is the mean ionic activity coefficient, ϕ is the osmotic coefficient, h^{sol} is the enthalpy of solution and $v_{\pm}$ is the apparent molar volume.

Optimisation point	$\gamma_{\pm}^{m}$ sOF	ϕ sOF	h^{sol} sOF	$v_{\pm}$sOF	Total OF
Optimisation starting model	7.54	1.56	4.08	4.22	17.40
Optimum model	1.97	0.44	4.70	0.25	7.35

As can be seen in Table 6, at the initial model of optimisation the contribution of the enthalpy of solution is lower than that of the mean ionic activity coefficient and apparent molar volume, but maintains the same order of magnitude. On the other hand, when we focus on the optimal model, it can be seen that even though the weight of the enthalpy of solution series is much lower than that of the mean ionic activity coefficient, this property ends up being the one that generates the largest contribution to the total objective function. Its value is in fact higher than it was at the starting point, illustrating that it is very difficult to minimize all properties simultaneously. This unexpected behaviour could point to inaccuracies in the model. As discussed below, it appears that the reason for this increase in the objective function is that the enthalpy of solution data are at low temperature (278-308 K) whereas the other data (mean ionic activity coefficient, and especially osmotic coefficients) are in a very different temperature range (up to 573 K). The model is unable to capture simultaneously the upward going slope at low temperature and the downward slope at high temperature (see Figure 4). In what follows, we will also use the average absolute relative deviation (AARD) of each data series (j), defined as:

$$AARD_j(\%) = \frac{1}{Npt_j}\sum_{i=1}^{Npt_j}\left(\frac{\left|D_{calc}^{i,j} - D_{exp}^{i,j}\right|}{D_{exp}^{i,j}}\right)\cdot 100\% \qquad (49)$$

4.2 Optimisation strategies

The number of possible parameters in the models presented is rather large. In a first step, it is decided to investigate all of them. A number of criteria are considered to investigate the quality of the results. Firstly, the deviations (AARD) must be small (< 10%) for each property. This first criterion imposes a stringent test as we use four different types of properties, each one providing a different sensitivity to the model. The second criterion is based on the physical meaning of the parameters. In contrast with empirical models, the SAFT family of models are based on molecular models that imply some restrictions on the parameter values. Finally, the sensitivity of the global objective function, and of each individual property within the objective function towards the parameter values is investigated. This sensitivity analysis will allow us to reduce the number of parameters.

Two strategies are used to carry out the optimisations. The parameters and their possible restrictions are presented in Table 7. In strategy “a” all available parameters are adjusted. For the dispersive models, the interactions between the ions and the solvent, as well as the interactions between the ions (cation-cation, anion-anion and cation-anion) are taken into account. For associative models, interactions between ions of same charge are not allowed in the framework. In strategy “b”, only 3 parameters are used for both dispersive and associative models. The discussion of why these parameters have been set in strategy “b” is presented below.

Table 7 : Unitary and binary parameters used for the optimisation strategies "a" and "b" ▫. Both strategies are applied for both dispersive and associative models. σ_i^{HS}, σ_i^{MSA} and σ_i^{Born} are the hard sphere, MSA and Born diameters, respectively, $\alpha_{0,\text{ion}}$ and $\alpha_{T,ion}$ are the adjustable parameters of the Simonin dielectric constant, ε_{ij} is the dispersion energy, ε_{ij}^{AB} is the association energy and k_{ij}^{AB} is the association volume.

Strategy	"a"	"b"
Unary parameters (both types of model)		
σ_i^{HS}	Variable	Variable
σ_i^{MSA}	Variable	Fixed**
σ_i^{Born}	Fixed (see section 3.6)	
${\alpha_{0,ion}}^*$	Variable see section 3.7*	0
${\alpha_{T,ion}}^*$		
Binary parameters for dispersive models (models type 1)		
$\varepsilon_{water-Water}$	Fixed	Fixed
$\varepsilon_{Na-Water}$	Variable	Fixed
$\varepsilon_{Cl-water}$	Variable	Fixed
ε_{Na-Na}	Variable	0
ε_{Cl-Cl}	Variable	0
ε_{Na-Cl}	Variable	Variable
Binary parameters for associative models (models type 2)		
$\varepsilon_{water-Water}^{AB}$	Fixed	Fixed
$\varepsilon_{Na-Water}^{AB}$	Variable	Variable
$\varepsilon_{Cl-water}^{AB}$	Variable	Fixed
ε_{Na-Cl}^{AB}	Variable	Variable
ε_{Na-Na}^{AB}	0	0
ε_{Cl-Cl}^{AB}	0	0
$k_{Na-Water}^{AB}$	Variable	0.044
$k_{Cl-water}^{AB}$	Variable	0.044
k_{Na-Cl}^{AB}	Variable	0.044
k_{Na-Na}^{AB}	0	0
k_{Cl-Cl}^{AB}	0	0
Number of parameters		
Model 1.0, 1.1	9	3
Model 1.2	11	
Model 2.0, 2.1	10	3
Model 2.2	12	

*Used only for models 1.2 and 2.2

** See equation (54).

▫ In the dispersive models only the association energy between water molecules is taken into account, the other association interactions are equal to 0. For the associative models only the dispersion energy between water molecules is considered, all other dispersion interactions are set to zero.

4.3 Results

4.3.1 Models type 1 (dispersive models)

a. Strategy "a"

In Table 8 the AARD (%) obtained with the optimisation strategy "a" applied to dispersive models are presented. It can be observed that the deviations for the different properties are not of the same order of magnitude. The deviations on the enthalpy of solution are often much larger than those for the other

properties. None of the dispersive models investigated in this work are able to reproduce quantitatively the downward trend of the enthalpy of solution with molality (see Figure 6). This is related to the fact that none of the models can reproduce accurately the low temperature increasing behaviour of the mean ionic activity coefficient with temperature. Indeed, as shown further, the only model that yields qualitatively good results for the enthalpy of solution, also shows a correct behaviour of the mean ionic activity coefficient with respect to temperature.

Table 8 : Average absolute relative deviation (AARD) of the optimisations of dispersive models using optimisation strategy "a" (model 1.2' is discussed in section 4.3.1-III). $\gamma_{\pm}^{m}$ is the mean ionic activity coefficient, ϕ is the osmotic coefficient, h^{sol} is the enthalpy of solution and $v_{\pm}$ is the apparent molar volume. In bold the results of the model with the lowest AARD.

	Model 1.0 $AARD_j$ / %	Model 1.1 $AARD_j$ / %	Model 1.2 $AARD_j$ / %	*Model 1.2' $AARD_j$ / %*
$\gamma_{\pm}^{m}$	3.53	3.36	**3.10**	3.33
ϕ	5.72	5.15	**4.82**	5.70
h^{sol}	37.94	38.22	**37.44**	36.37
$v_{\pm}$	6.61	5.44	**5.72**	5.43

Osmotic coefficients and mean ionic activity coefficients are related through the Gibbs-Duhem relationship. Yet, the data on osmotic coefficients are available at much higher temperature and concentration. Therefore, the deviations on the osmotic coefficients are an indication of the capacity of the model to extrapolate both towards high temperatures and concentrations. The apparent molar volumes provide a detailed view on the quality for the molar density of the models. For this property, deviations below 10% can be considered acceptable. In Table 8, the model 1.2 which leads to the lowest deviations is highlighted in bold. The results obtained with models 1.0 and 1.2 are similar except for the deviation in the apparent molar volume.

As shown in Figure 5, using model 1.2 it is possible to represent accurately the mean ionic activity coefficient with respect to the salt concentration. However, the model results in a continuous decrease of the MIAC with respect to temperature. Therefore, a positive slope of the enthalpy of solution is observed (see Figure 6). The osmotic coefficients and apparent molar volume are both well represented qualitatively and quantitatively (see supplementary information A). Graphs showing the detailed contribution of each term to the natural logarithm of mean ionic activity coefficient at 298 K, and the behaviour of the different dielectric constants models with respect to temperature and salt concentration are provided in supplementary information B and C.

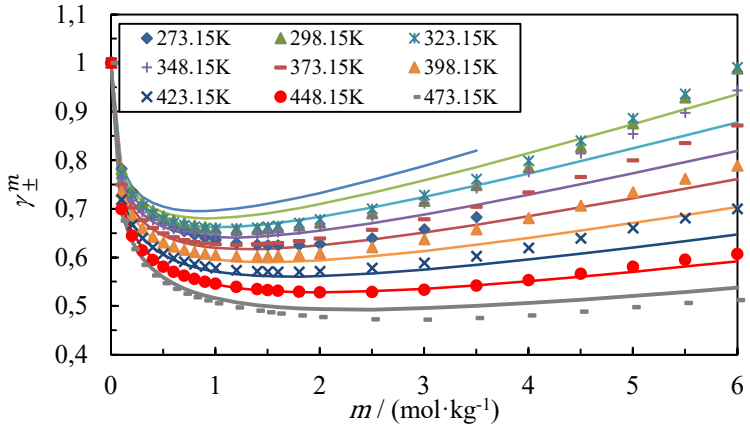

Figure 5 : NaCl mean ionic activity coefficient ($\gamma_{\pm}^{m}$) as a function of salt concentration obtained from the optimisation of model 1.2 using optimisation strategy "a". The symbols represent the experimental data and the curves show the results obtained with the model. The calculations were made at 1 bar for temperatures up to 373.15 K, the saturation pressure of the solvent was used for temperatures above 373.15 K.

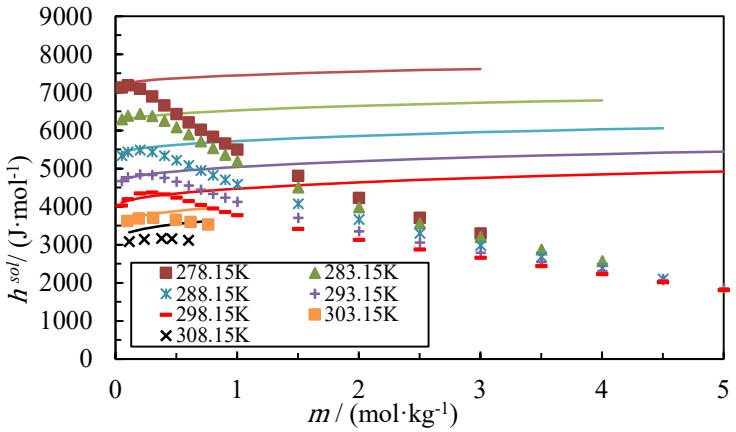

Figure 6 : NaCl enthalpy of solution as a function of salt concentration obtained from the optimisation of model 1.2 using optimisation strategy "a". The symbols represent the experimental data and the curves represent the results obtained with the model. The calculations were made at 1 bar.

Since the final objective of this study is to obtain a model that is consistent with the physics of the electrolytic solutions, it is important to verify that the adjusted parameters make sense from a physical point of view. In Table 9 the parameters obtained for the different models with optimisation strategy "a" are shown.

Three different criteria are used to analyse parameter consistency:

I. The first criterion is based on the comparison between MSA diameter and hard sphere diameter.

As MSA diameter (σ_i^{MSA}) can be seen as a hydrated ion diameter, it must be bigger or equal to the hard sphere diameter (σ_i^{HS}). In addition, the hard sphere diameter of the cation ($\sigma_{Na^+}^{HS}$) must be smaller than the hard sphere diameter of the anion ($\sigma_{Cl^-}^{HS}$), following the conclusion of several fundamental studies [69, 70].

Table 9 : Parameters obtained of the optimisation of dispersive models using the optimisation strategy "a". In bold, inconsistencies regarding diameters and energy parameters (discussed below). ε_{ij} is the dispersion energy, σ_i^{HS}, σ_i^{MSA} and σ_i^{Born} are the hard sphere, MSA and Born diameters respectively, $\alpha_{0,ion}$ and $\alpha_{T,ion}$ are the adjustable parameters of the Simonin dielectric constant.

Parameters	Model 1.0	Model 1.1	Model 1.2	Model 1.2'
$\varepsilon_{water-Water}/k_B$/ K			201.75	
$\varepsilon_{Na-Water}/k_B$/ K	392.25	370.79	570.16	590.59
$\varepsilon_{Cl-water}/k_B$/ K	379.82	427.55	257.40	287.46
ε_{Na-Cl}/k_B/ K	332.29	721.46	709.67	794.42
ε_{Na-Na}/k_B/ K	477.09	148.57	**651.02**	**763.48**
ε_{Cl-Cl}/k_B/ K	720.61	492.07	343.50	366.24
$\varepsilon^{AB}_{water-Water}/k_B$ / K			1813.00	
σ_{Na}^{HS} / Å	3.22	3.42	3.59	3.76
σ_{Cl}^{HS} / Å	**2.81**(1)	**2.64**(1)	**2.53**(1)	**2.31**(1)
σ_{Na}^{MSA} / Å	**1.59**(2)	**1.40**(2)	**3.34** (2)	4.03
σ_{Cl}^{MSA} / Å	7.49	5.11	4.09	3.50
σ_{Na}^{Born}/ Å			3.23	
σ_{Cl}^{Born}/ Å			4.51	
$\alpha_{0,ion}$	-	-	0.013	0
$\alpha_{T,ion}$	-	-	-0.001	0

[a] In dispersive models only water-water association interactions are taken into account. The Born diameter has been fixed for all models using the values presented in Table 4 (see section 3.6). Water-water dispersion and association energies are also fixed [9].

(1) $\sigma_{Cl}^{HS}<\sigma_{Na}^{HS}$

(2) $\sigma_{Na}^{MSA} < \sigma_{Na}^{HS}$

In Table 9, the diameters that do not meet the above conditions are highlighted in bold. As can be seen in the table, none of the models have physically consistent diameters. However, with model 1.2' only one diameter is inconsistent. This may suggest firstly that there are several local minima, and secondly that using the salt concentration explicitly within the dielectric constant, may lead to problems of consistency between the parameters.

II. The second criterion is based on the interaction energies:

As a second consistency test, it is checked whether the attractive interaction parameters between the like charge ions are physically consistent. The potential energy as a function of the distance may be evaluated as the sum of a square well (SW) and a coulombic (Coulomb) interaction:

$$u(r_{ij}) = u(r_{ij})^{SW} + u(r_{ij})^{Coulomb} \tag{50}$$

The square-well ($u(r_{ij})^{SW}$) and the Coulomb ($u(r_{ij})^{Coulomb}$) potential are given by [25, 61] as follows:

$$u(r_{ij})^{SW} = -\varepsilon_{ij} \qquad when \qquad \sigma_{ij}^{HS} < r_{ij} < \lambda\sigma_{ij}^{HS} \tag{51}$$

$$u(r_{ij})^{Coulomb} = \frac{z_i z_j e^2}{4\pi\varepsilon_o\varepsilon_r r_{ij}} \tag{52}$$

A negative (attractive) interaction energy can only be observed when the intermolecular distance lies between σ_{ij}^{HS} and $\lambda\sigma_{ij}^{HS}$. The parameter λ is the well width and can be taken at 1.2 or 1.5 depending on the authors [20, 71], in this study λ is equal to 1.2. For two ions of the same charge not to attract each other, the potential energy must be always greater than or equal to 0. Applying these conditions and combining equations (50), (51) and (52) yields:

$$\varepsilon_{ij} \leq \frac{z_i z_j e^2}{4\pi\varepsilon_o\varepsilon_r\lambda\sigma_{ij}^{HS}} \tag{53}$$

Equation (54) can be used to assess whether the parameters obtained for the dispersion energies would not lead to an unphysical attraction of ions of the same charge. If the ion-ion dispersion energy is bigger than the one obtained from equation (54), the parameters are rejected. By applying this analysis to the results obtained in Table 9, it was observed that the models 1.2 and 1.2' present inconsistent parameters. In both cases cation-cation attractive interaction is obtained (bold parameters in Table 9). Therefore, no dispersive model presented here is physically consistent. This proves that even if a model can represent experimental data accurately, it does not mean that it is physically correct. Some authors such as Held et al. [72, 73] have used optimisation strategies in which they cancel interactions between like-charged ions. By this way, the consistency problem presented above is solved.

III. The third criterion is based on the dielectric constant

In Figure 7 the water dielectric constant calculated by each of the three models as a function of salt concentration is shown. For the calculation of the Simonin dielectric constant, the parameters presented in Table 9 were used. As can be seen in Figure 7, both the Schreckenberg and Simonin models generate very similar results for the dielectric constant. On the other hand, the Pottel model is more sensitive to the variation of the salt concentration and differs significantly from the two other models. This is because the parameter values of the Simonin model are very small, which may indicate that the system tends to eliminate the impact of salt concentration within the Simonin dielectric constant. Note that the Schreckenberg model shows a decreasing trend of the dielectric constant with molality, even though the salt mole fraction does not appear in equation (40). It is related to the decrease of the ratio $n_{solvent}/V$. As will be shown later (in section 4.3.2) this tendency is repeated for the associative models, where the best results are obtained with the model 2.0 (Schreckenberg model for dielectric constant). The behaviour of the different dielectric constants with respect to salt concentration and at different temperatures is presented in supplementary information C.

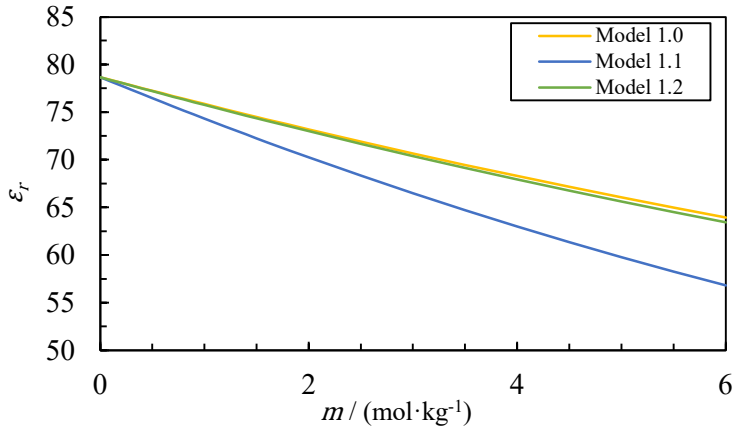

Figure 7 : Dielectric constant as a function of NaCl concentration at 298.15 K, using the parameters presented in Table 9 for the three dispersive models 1.0 (Schreckenberg), 1.1 (Pottel) and 1.2 (Simonin).

It is interesting to consider why, considering that the only difference between the models is the dielectric constant, and that this property is almost identical in models 1.0 and 1.2, the parameters values and the AARD % should also be very similar. In Table 8 the deviations shown are of the same order for the two models, except for apparent molar volume. Yet the parameters values are very different. This is most probably because local minima that have been reached resulting from parameter degeneracy. When regressing the parameters again (using the parameters of model 1.2 as a starting point for optimisation, and setting $\alpha_{0,ion} = 0$ and $\alpha_{T,ion} = 0$, which is equivalent to model 1.0), new parameters are obtained with values close to the parameters of model 1.2 (see Table 9). The deviations are shown in Table 8 (model 1.2'). It appears that the deviations are similar, but even smaller than those obtained with model 1.2, confirming that (1) there are local minima, and that (2) this approach is the one to be recommended.

b. Strategy "b"

The goal of strategy "b" is to reduce the number of adjustable parameters. A global sensitivity analysis was performed on the optimal solution of strategy "a" (model 1.2). It allows visualizing how much the objective function is affected by a variation on any given input parameter. This analysis is performed by analysis of variance and Monte-Carlo sampling is used to construct response surfaces of each objective function [74].

From the sensitivity analysis the three most important parameters for the dispersive models are found to be the hard sphere diameters of both ions and the dispersion energy between the cation and the anion. Therefore, these three parameters are the only ones used in regression strategy "b". Taking advantage of the fact that the MSA diameters are not as sensitive and to reduce the number of adjustable parameters, a proportionality parameter between the hard sphere and the MSA diameters is introduced as:

$$\sigma_i^{MSA} = \sigma_i^{HS} \cdot 1.5 \tag{54}$$

Using the arguments developed above, a second optimization is performed with a reduced number of parameters (strategy "b" in Table 7). As shown in Table 10, after reducing the number of parameters from 11 to 3 the results have not worsened greatly. An increase in the deviation of no more than 3% is obtained, except for the case of the apparent molar volume, for which it increases by almost 3.5%. The deviation increases in the osmotic coefficient and in the enthalpy of solution are larger than in the mean ionic activity coefficient. This is a consequence of a deterioration of low enthalpy of solution and high temperature osmotic coefficient properties, as is also visible in Figure 8. It can be seen in the figure that the model can reproduce the mean ionic activity coefficient with respect to salt concentration, but unfortunately not the trend with respect to temperature. This is expected considering that the original model, with all parameters was also unable to reproduce the temperature dependence of the MIAC. A large deviation at low (273.15 K) and high (473.15 K) temperature is observed. The graphs of the results obtained for the other properties are presented in supplementary Information A.

Table 10 : Comparison between the best results obtained using optimisation strategy "a" (model 1.2 - 11 parameters), and the results obtained using optimisation strategy "b" (model 1.0 – 3 parameters).

Strategy	AARD$_j$ / %			
	$\gamma_{\pm}^{m}$	ϕ	h^{sol}	$v_{\pm}$
a (Model 1.2)	3.53	5.72	37.94	6.61
b (Model 1.0)	4.02	6.52	41.47	8.90

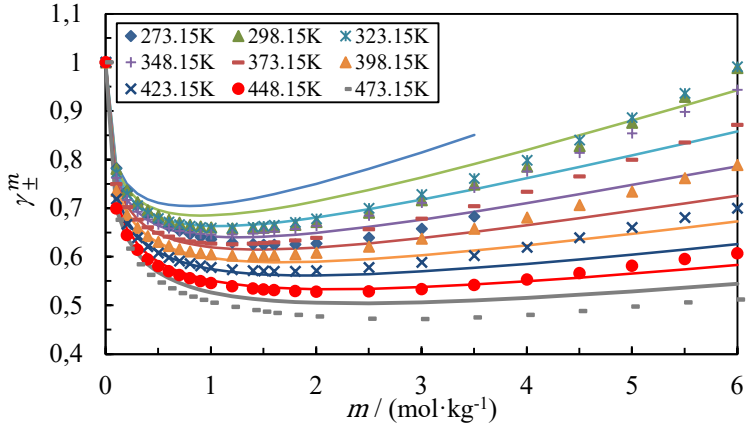

Figure 8 : NaCl mean ionic activity coefficient as a function of salt concentration obtained from the optimisation of model 1.0 using optimisation strategy "b". The symbols represent the experimental data and the curves the results obtained with the model. The calculations were made at 1 bar for temperatures up to 373.15 K, then the saturation pressure of the solvent was used for temperatures above 373.15 K.

The parameters obtained for model 1.0 using strategy "b" are shown in Table 11. The parameters used to optimise the model are in bold.

Table 11 : Parameters obtained from the optimisation of model 1.0 using optimisation strategy "b" [a]. Regressed parameters are in bold. ε_{ij} is the dispersion energy, ε_{ij}^{AB} is the association energy, σ_i^{HS}, σ_i^{MSA} and σ_i^{Born} are the hard sphere, MSA and Born diameters respectively.

Parameter	value	Parameter	value
$\varepsilon_{water-Water}/k_B$/ K	201.75	σ_{Na}^{HS} / Å	**2.74**
$\varepsilon_{Na-Water}/k_B$/ K	201.75	σ_{Cl}^{HS} / Å	**2.84**
$\varepsilon_{Cl-water}/k_B$/ K	201.75	σ_{Na}^{MSA} / Å	3.14
ε_{Na-Cl}/k_B/ K	**56.79**	σ_{Cl}^{MSA} / Å	5.17
ε_{Na-Na}/k_B/ K	0.00	σ_{Na}^{Born}/ Å	3.23
ε_{Cl-Cl}/k_B/ K	0.00	σ_{Cl}^{Born}/ Å	4.51
$\varepsilon_{water-Water}^{AB}/k_B$ / K	1813.00		

[a] In dispersive models only water-water association interactions are taken into account. Ion-water dispersion energies are fixed with a value equal to the water-water dispersion energy. Cation-cation and anion-anion dispersion energies are set to 0. The MSA diameter is calculated using equation 54. Born diameter has been fixed using the values presented in Table 4 (see section 3.6). Water-water dispersion and association energies are also fixed [9].

As a conclusion for the dispersive models, it is possible to reach reasonable accuracy on the investigated properties, with the exception of the temperature-dependence of mean ionic activity coefficient (and consequently on enthalpy of solution). It is thus shown that the number of parameters can be reduced without greatly affecting the quality of the model.

4.3.2 Models type 2 (Associative models)

For the case of the associative-type models, the same procedure described in the previous section for the dispersive models is applied.

a. Strategy "a"

Using this strategy, the number of parameters is very large (see Table 7: 10 to 12 parameters).

Table 12 : Absolute relative deviation (ARD) from the optimisations of associative models using optimisation strategy "a". $\gamma_{\pm}^{m}$ is the mean ionic activity coefficient, ϕ is the osmotic coefficient, h^{sol} is the enthalpy of solution and $v_{\pm}$ is the apparent molar volume. In bold the results of the model with the lowest ARD.

	Model 2.0 $AARD_j$ / %	Model 2.1 $AARD_j$ / %	Model 2.2 $AARD_j$ / %
$\gamma_{\pm}^{m}$	**1.02**	2.07	1.63
ϕ	**2.97**	2.49	1.60
h^{sol}	**16.99**	31.54	23.15
$v_{\pm}$	**4.96**	8.58	5.70

In Table 12 the AARD (%) obtained with optimisation strategy "a" applied to the associative models are shown, and in Table 13 the corresponding parameters are presented. As shown in Figure 9, model 2.0 leads to a very accurate representation of the mean ionic activity coefficient with respect to not only salt concentration, but also temperature, in contrast to dispersive models. This same type of behaviour is found in model 2.2, but with lower accuracy. In contrast, model 2.1 only reproduces the behaviour of the mean ionic activity coefficient with respect to the salt concentration. As can be seen in Table 12, the deviation of the enthalpy of solution of model 2.1 is almost twice the deviation of model 2.0.

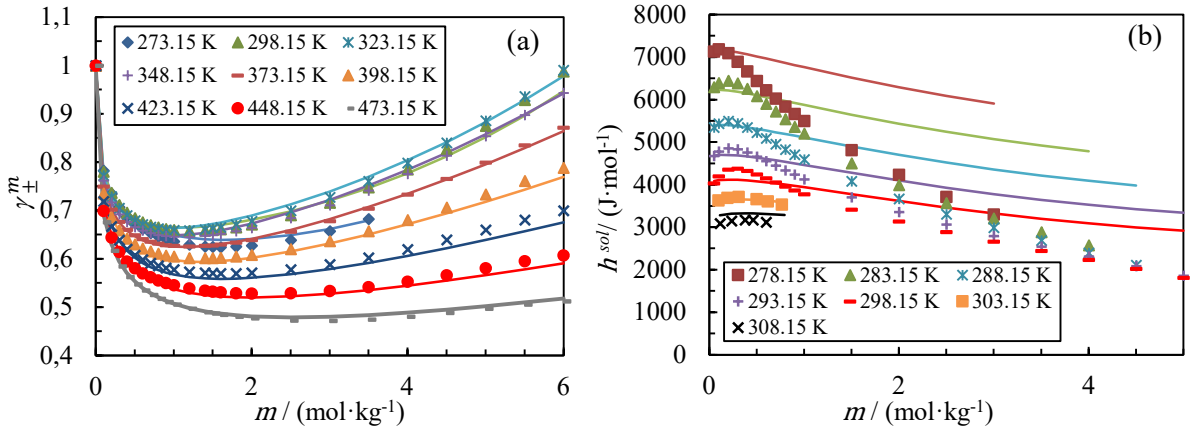

Figure 9 : (a) NaCl mean ionic activity coefficient and (b) enthalpy of solution as a function of the salt concentration obtained from the optimisation of model 2.0 using optimisation strategy "a". The symbols represent the experimental data and the curves represent the results obtained with the model. The calculations were made at 1 bar for temperatures up to 373.15 K, then the saturation pressure of the solvent was used for temperatures above 373.15 K.

In Figure 9 and Figure 10 the mean ionic activity coefficient and enthalpy of solution results for models 2.0 and 2.1, respectively, are shown. In Figure 9, it can be gleaned that model 2.0 can reproduce qualitatively the behaviour of the enthalpy of solution with respect to the salt concentration. In contrast, model 2.1 does not reproduce this behaviour (see Figure 10). The relationship between the slope of enthalpy of solution curve and the temperature behaviour of the mean ionic activity coefficient was pointed out theoretically in section 2.4. Here, it can be seen that the model correctly follows the theory: only model 2.0, that has the correct enthalpy of solution slope is able to follow the mean ionic activity coefficient trend with a maximum value close to 323 K.

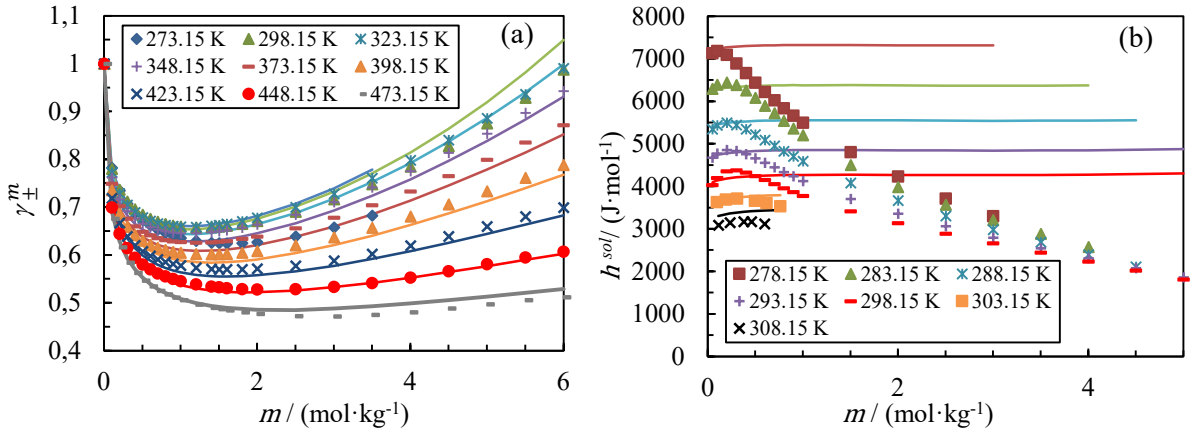

Figure 10 : (a) NaCl mean ionic activity coefficient and (b) enthalpy of solution as a function of salt concentration obtained from the optimisation of model 2.1 using optimisation strategy "a". The symbols represent the experimental data and the curves represent the results obtained with the model. The calculations were made at 1 bar for temperatures up to 373.15 K, then the saturation pressure of the solvent was used for temperatures above 373.15 K.

As with the dispersive models, the parameters are checked for their physical consistency. In Table 13 a summary of the parameters obtained for the associative models with the optimisation strategy "a" are shown. Due to the association scheme proposed, the interaction between two ions is only possible if they are of different charges. Thus, in contrast to dispersive models, associative models do not consider short range cation-cation and anion-anion interactions. Hence, the physical consistency analysis focuses only on adjusted diameters, with the same criterion as for dispersive model analysis.

Table 13 : Parameters obtained from the optimisation of associative models using the optimisation strategy "a" [a]. In bold, inconsistencies regarding diameters. ε_{ij}^{AB} is the association energy, $k_{Na-Water}^{AB}$ is the association volume, σ_i^{HS}, σ_i^{MSA} and σ_i^{Born} are the hard sphere, MSA and Born diameters respectively, $\alpha_0 ion$ and $\alpha_T ion$ are the adjustable parameters of the Simonin dielectric constant.

Parameters	Model 2.0	Model 2.1	Model 2.2
$\varepsilon_{water-Water}/k_B$ / K		201.61	
$\varepsilon_{Na-Water}^{AB}/k_B$ / K		1813.00	
$\varepsilon_{Na-Water}^{AB}/k_B$ / K	2132.21	2450.28	1762.99
$\varepsilon_{Cl-Water}^{AB}/k_B$ / K	2319.02	1994.12	2981.09
$\varepsilon_{Na-Cl}^{AB}/k_B$ / K	2410.64	2100.38	871.87
$k_{Na-Water}^{AB}$	0.005	0.064	0.003
$k_{Cl-water}^{AB}$	0.02	0.003	0.016
k_{Na-Cl}^{AB}	0.002	0.002	0.001
σ_{Na}^{HS} / Å	1.00	1.42	4.08
σ_{Cl}^{HS} / Å	4.17	4.32	**2.01**[(3)]
σ_{Na}^{MSA} / Å	5.86	**1.00**[(2)]	3.97
σ_{Cl}^{MSA} / Å	**2.00** [(1)]	6.24	6.64
σ_{Na}^{Born} / Å		3.23	
σ_{Cl}^{Born} / Å		4.51	
$\alpha_0 ion$	-	-	-0.047
$\alpha_T ion$	-	-	-0.003

[a] In associative models only water-water dispersion interactions are taken into account. Born diameter has been fixed for all models using the values presented in Table 4 (see section 3.6). Water-water dispersion and association energies are also fixed [9].

(1) $\sigma_{Cl}^{MSA} < \sigma_{Cl}^{HS}$

(2) $\sigma_{Na}^{MSA} < \sigma_{Na}^{HS}$

(3) $\sigma_{Cl}^{HS} < \sigma_{Na}^{HS}$

In Table 13 the diameters that do not meet the consistency criterion are highlighted. None of the models have physically consistent parameters. It should be noted that all parameters that are not physically

consistent reach the lower limit imposed in the optimisations. This may be an indicator that the models are over-parameterised. Sensitivity analysis has therefore been used to verify the impact of the parameters on the objective function, and to reduce the number of parameters used for optimisation in strategy "b".

b. **Strategy "b"**

As for dispersive model, the parameters $\alpha_{0,ion}$ and $\alpha_{T,ion}$ are close to zero, indicating again that taking explicitly into account salt effect in dielectric constant has no real effect on the results. The sensitivity analysis is focused on model 2.0, which leads to the best results in strategy "a". Similar conclusion is reached as for dispersive models, in that the most influential parameters are the hard sphere diameters and the interaction energy between cation and anion. In contrast to the dispersive models, the energy of association between cation and water is also found to have an important impact on the objective function. Therefore, the parameterization can be limited to 4 parameters. This is further reduced by considering that the response surface of the hard sphere diameters (Figure 11) highlights a correlation between the diameters.

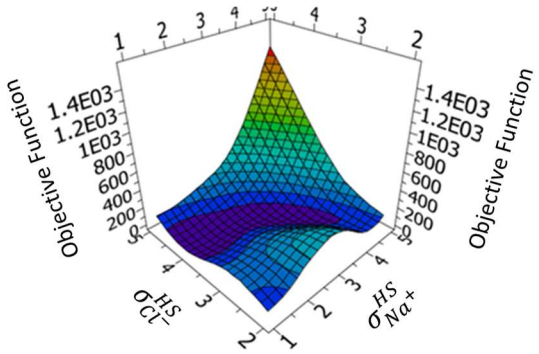

Figure 11 : Response surface showing the effect of the hard sphere diameters on the total objective function

In addition, in Figure 11 that the experimental Pauling diameter of the cation (1.9 Å) is located in a reasonably flat zone. For this reason, the value of the cation hard sphere diameter is set equal to the Pauling diameter. Finally, association volumes are observed to have a poor impact on the objective function, compared to other parameters. To reduce the number of adjustable parameters, their values are fixed to that of water, as was done in previous studies [9, 11]. As in dispersive models, the MSA diameter does not have a high impact on the objective function and is fixed using equation (54). Strategy "b" summarized in Table 7 is now applied to model 2.0.

Table 14 : Comparison of the best results obtained using optimisation strategy "a" (model 2.0 - 10 parameters), with the results obtained using optimisation strategy "b" (model 2.0 – 3 parameters). $\gamma_{\pm}^{m}$ is the mean ionic activity coefficient, ϕ is the osmotic coefficient, h^{sol} is the enthalpy of solution and $v_{\pm}$ is the apparent molar volume.

Strategy	AARD$_j$ / %			
	$\gamma_{\pm}^{m}$	ϕ	h^{sol}	$v_{\pm}$
a (Model 2.0)	1.02	2.97	16.99	4.96
b (Model 2.0)	3.56	5.61	34.58	14.01

There are now only 3 parameters left, which are association energy cation-solvent ($\varepsilon^{AB}_{Na-Water}/k_B$), cation-anion association energy ($\varepsilon^{AB}_{Na-C}/k_B$) and anion hard sphere diameter (σ^{HS}_{Cl}). In Table 14 the comparison of the AARD results of model 2.0 using optimisation strategy "a" and "b" are compared. The deviations are similar for the mean ionic activity coefficient and osmotic coefficient (difference less than 3% in both cases). However, the ARD for enthalpy of solution is more than double and almost triple for apparent molar volume. In Figure 12 the quality of this new model is seen. The model can describe the mean ionic activity coefficient as a function of concentration, but only at intermediate temperatures, and incapable to capture the slope of enthalpy of solution. The increase in the deviation of the apparent molar volume can be attributed to the fact that in strategy "b", only the hard sphere

diameter of the anion has been optimised, while this property is strongly dependent on the hard sphere diameter of both ions.

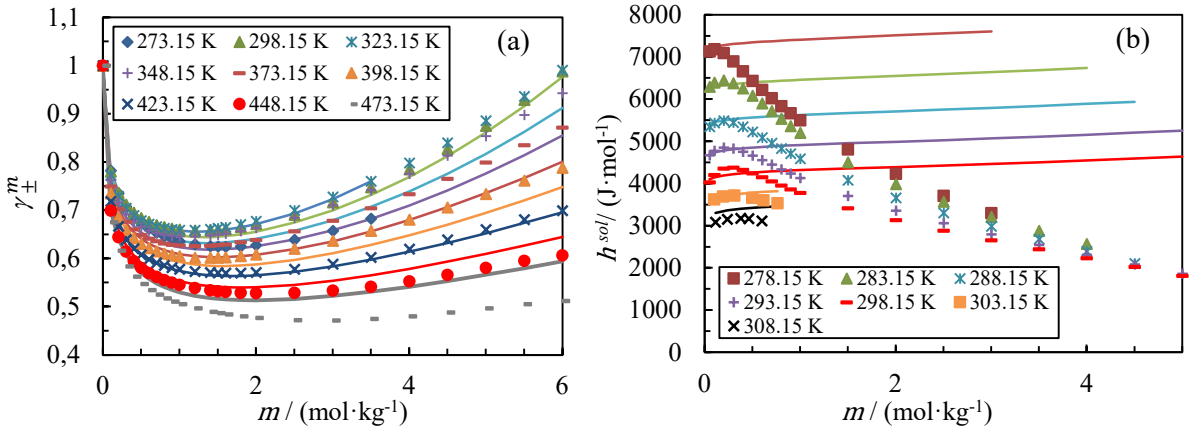

Figure 12 : (a) Mean ionic activity coefficient and (b) enthalpy of solution as a function of salt concentration obtained from the optimisation of model 2.0 using optimisation strategy "b". The symbols represent the experimental data and the curves represent the results obtained with the model. The calculations were made at 1 bar for temperatures up to 373.15 K, then the saturation pressure of the solvent was used for temperatures above 373.15 K.

Table 15 presents the parameter values obtained for model 2.0 using strategy "b". In bold the parameters used to optimise the model.

Table 15 : Parameters obtained from the optimisation of model 1.0 using optimisation strategy "b" [a]. Only bold parameters are regressed. ε_{ij}^{AB} is the association energy, $k_{Na-Water}^{AB}$ is the association volume, σ_i^{HS}, σ_i^{MSA} and σ_i^{Born} are the hard sphere, MSA and Born diameters respectively.

Parameter	value	Parameter	value
$\varepsilon_{water-Water}^{AB}/k_B$ / K	1813.00	$\varepsilon_{water-Water}/k_B$ / K	201.61
$\varepsilon_{Na-Water}^{AB}/k_B$ / K	**2617.86**	σ_{Na}^{HS} / Å	1.9
$\varepsilon_{Cl-Water}^{AB}/k_B$ / K	1813.00	σ_{Cl}^{HS} / Å	**3.96**
$\varepsilon_{Na-Cl}^{AB}/k_B$ / K	**2047.78**	σ_{Na}^{MSA} / Å	2.85
$k_{Na-Water}^{AB}$	0.044	σ_{Cl}^{MSA} / Å	5.94
$k_{Cl-water}^{AB}$	0.044	σ_{Na}^{Born} / Å	3.23
k_{Na-Cl}^{AB}	0.044	σ_{Cl}^{Born} / Å	4.51

[a] In associative models only water-water dispersion interactions are taken into account. Anion-water association energy, ion-water association volume and cation-anion association volume are fixed with a value equal to the water-water association energy and water-water association volume respectively. The cation hard sphere diameter is fixed with the Pauling diameter. The MSA diameter is calculated using equation 54. Born diameter has been fixed using the values presented in Table 4 (see section 3.6). Water-water dispersion and association energies are also fixed [9].

As a conclusion on the use of associative models, it appears that the large number of parameters makes it possible to reach a very nice representation of the data, but at the price of non-physical parameters. The most important parameters are the cation-anion interaction energy. It is observed that when the number of parameters is reduced in such a way as to make the order of the diameters physically meaningful, it becomes impossible to represent correctly the enthalpy of solution and the temperature trend of the mean ionic activity coefficient.

5 Discussion

Having settled on two modelling approaches that provide equivalent results, we can now evaluate their behavior on various salts and properties. In this section, we first evaluate how the model can be extrapolated to other salts. We then present how the use of the full model impacts the Gibbs energy of solvation and finally, some discussion is proposed on single ionic activity coefficients. The salts considered are NaCl, KCl, NaBr and KBr. In Table 16 the temperature and concentration range of the experimental data used for each salt are presented.

Table 16 : Number of experimental data points (Npt^j), temperature and concentration range of each property used for the optimizations of models 1.0 and 2.0 ¤. $\gamma_{\pm}^{m}$ is the mean ionic activity coefficient, ϕ is the osmotic coefficient, h^{sol} is the enthalpy of solution and $v_{\pm}$ is the apparent molar volume.

Salt		$\gamma_{\pm}^{m}$	ϕ	h^{sol}	$v_{\pm}$	Reference
KCl	Npt^j	82	120	64	75	[75–82]
	Temperature range / K	273.15-323.15	273.15-413.15	298.15-348.15	273.15-323.15	
	Molality range / mol.kg^{-1}	0 - 4.5	0 - 5.2	0 - 0.6	0.3 - 1	
NaBr	Npt^j	133	233	17	24	[67, 83–86]
	Temperature range / K	273.15-333.15	298.15-498.15	298.15-333.15	298.15	
	Molality range / mol.kg^{-1}	0 - 9.5	0 - 10.6	0 - 0.2	0 - 8.3	
KBr	Npt^j	29	286	52	52	[43, 67, 84, 86–88]
	Temperature range / K	298.15	298.15-498.15	283.15-313.15	313.15-553.15	
	Molality range / mol.kg^{-1}	0 - 5.5	0 - 7.5	0 - 6	0.1 - 1.5	

¤ Uncertainty ($err(\%) - e^j$) and data serial weight (w_s^j) are the same for all salts and are presented in Table 5.

5.1 Model extension to 4 salts

Using the approaches chosen in the previous section, an extension has been made to model the same properties in aqueous solution of 4 salts, using the strategy "b" previously described (3 adjustable parameters). The deviations with respect to the data whose references and those provided in Tables 1 and 16 are given in Table 17. The resulting parameters from the model optimisation are shown in Table 18. Note that the parameters for NaCl have been re-optimised. This was done to find parameters that work well for salts that share the same ions (NaCl, KCl, NaBr).

Table 17 : Absolute relative deviations (ARD) from optimisation of models 1.0 and 2.0 using optimisation strategy "b". $\gamma_{\pm}^{m}$ is the mean ionic activity coefficient, ϕ is the osmotic coefficient, h^{sol} is the enthalpy of solution and $v_{\pm}$ is the apparent molar volume.

	Model 1.0 (Dispersive model)				Model 2.0 (Associative model)			
	NaCl	KCl	NaBr	KBr	NaCl	KCl	NaBr	KBr
	AARD$_j$ / %							
$\gamma_{\pm}^{m}$	3.98	3.56	6.17	3.53	3.90	1.54	5.53	1.16
ϕ	6.18	4.14	7.60	6.03	7.19	1.42	7.70	2.19
h^{sol}	42.16	1.16	2.95	7.54	40.46	1.06	2.83	5.53
$v_{\pm}$	6.86	6.23	22.26	6.06	10.90	36.23	39.22	4.06

Table 18 : Parameters obtained from the optimisation of model 1.0 and 2.0 using optimisation strategy "b", for aqueous NaCl, KCl, NaBr and KBr [a]. Only bold parameters are regressed. σ_i^{HS}, σ_i^{MSA} and σ_i^{Born} are the hard sphere, MSA and Born diameters respectively. ε_{ij} is the dispersion energy, ε_{ij}^{AB} is the association energy, $k_{Na-Water}^{AB}$ is the association volume.

	Model 1.0 (Dispersive model)				Model 2 (Associative model)			
Parameters	NaCl	KCl	NaBr	KBr	NaCl	KCl	NaBr	KBr
$\boldsymbol{\sigma_{cation}^{HS}}$ / Å	**2.11**	**3.46**	**2.11**	**3.46**	1.90	2.66	1.90	2.66
$\boldsymbol{\sigma_{anion}^{HS}}$ / Å	**3.32**	**3.32**	**3.48**	**3.48**	**3.84**	**3.84**	**3.69**	**3.69**
σ_{cation}^{MSA} / Å	4.34	4.15	4.34	4.15	2.85	3.99	2.85	3.99
σ_{anion}^{MSA} / Å	4.53	4.53	5.21	5.21	5.76	5.76	5.54	5.54
σ_{Na}^{Born} / Å					3.23			
σ_{Cl}^{Born} / Å					4.51			
$\varepsilon_{water-Water}/k_B$ / K					201.61			
$\varepsilon_{cat-Water}/k_B$ / K	201.61	201.61	201.61	201.61	-	-	-	-
$\varepsilon_{ani-water}/k_B$ / K	201.61	201.61	201.61	201.61	-	-	-	-
$\boldsymbol{\varepsilon_{cat-ani}/k_B}$ / K	**26.76**	**238.61**	**5.43**	**198.18**	-	-	-	-
$\varepsilon_{cat-cat}/k_B$ / K	0.00	0.00	0.00	0.00	-	-	-	-
$\varepsilon_{ani-ani}/k_B$ / K	0.00	0.00	0.00	0.00	-	-	-	-
$\boldsymbol{\varepsilon_{water-Water}^{AB}/k_B}$ / K					1813.00			
$\boldsymbol{\varepsilon_{cat-Water}^{AB}/k_B}$ / K	-	-	-	-	**1270.11**	**1531.28**	**1270.11**	**1531.28**
$\varepsilon_{ani-Water}^{AB}/k_B$ / K	-	-	-	-	1813.00	1813.00	1813.00	1813.00
$\boldsymbol{\varepsilon_{cat-ani}^{AB}/k_B}$ / K	-	-	-	-	**0.00**	**0.00**	**0.00**	**201.16**
$k_{cat-Water}^{AB}$	-	-	-	-	0.04	0.04	0.04	0.04
$k_{ani-water}^{AB}$	-	-	-	-	0.04	0.04	0.04	0.04
$k_{cat-ani}^{AB}$	-	-	-	-	0.04	0.04	0.04	0.04

[a] In dispersive model 1.0 only water-water association interactions are taken into account. In associative model 2.0 only water-water dispersion interactions are considered Ion-water dispersion energies are fixed with a value equal to the water-water dispersion energy. Cation-cation and anion-anion dispersion energies are set to 0. Anion-water association energy, ion-water association volume and cation-anion association volume are fixed with a value equal to the water-water association energy and water-water association volume respectively. The cation hard sphere diameter is fixed with the Pauling diameter. The MSA diameter is calculated using equation 54. Born diameter has been fixed using the values presented in Table 4 (see section 3.6). Water-water dispersion and association energies are also fixed [9].

Several observations can be made.

5.1.1 Regarding the comparison between the two models

The global observation is that the two models are equally able to represent the four salts considered: the deviations are generally of the same order of magnitude (up to 6% for mean ionic activity coefficient and up to 8% for osmotic coefficient). Regarding the enthalpy of solution, only the NaCl deviations are significant, which is easily explained by the fact that only for this salt, high concentration enthalpies of solution are available. Concerning apparent molar volume, those of KCl and NaBr seem particularly difficult to capture correctly. It is important to remember that the apparent molar volume expresses the change in the volume of the solution when salt is added, this property is very sensitive and generates very small values, so it is difficult to obtain low deviations. The sensitivity analysis performed for the NaCl aqueous solution showed that the apparent molar volume is particularly sensitive to the variation of the hard sphere diameter. This explains why higher ARDs are obtained with the 2.0 model, as in this model only the HS diameter of the anions was optimised.

5.1.2 Regarding the parameter values.

Vaque Aura *et al.* [29] discussed how the shape of the mean ionic activity coefficient curve illustrates the competing tendency of ion solvation (curve leans upward) and ion pairing (curve leans downward). In the SAFT models, this competition can be made visible by comparing respectively the ion-water and ion-ion interaction parameters. According to Vaque Aura et al., the order of most solvating (least pairing) to least solvating (most pairing) salts is as follows: NaBr > NaCl > KBr > KCl, this same trend can be seen in the experimental data at 298.15 K in Figure 13. Looking at the magnitude of the model

1.0 parameters, where only ion-pairing parameters have been allowed to change, it appears indeed that NaBr has the lowest ion-pair interaction energy, while KBr and KCl have the highest values, KCl showing the highest value. The trend of these parameters agrees with the conclusions of Vaque Aura et al. [29]. For model 2.0, the association parameters are fitted. Almost all ion pair parameters are zero, pointing to full dissociation, except for KBr. For this last salt, it is true that 201 K is extremely small, and can therefore be considered zero as well. Hence, for this model, the solvation (ion-water) parameters should be used as a guide. Yet, here the trend seems opposite: the salts that are expected to "solvate" more have a smaller cation-water interaction energy. This may be caused by the imposed value of the association energy of the anion with water, that is larger than the one that is found between cation and water. It is known that cations are more solvated than anions [37].

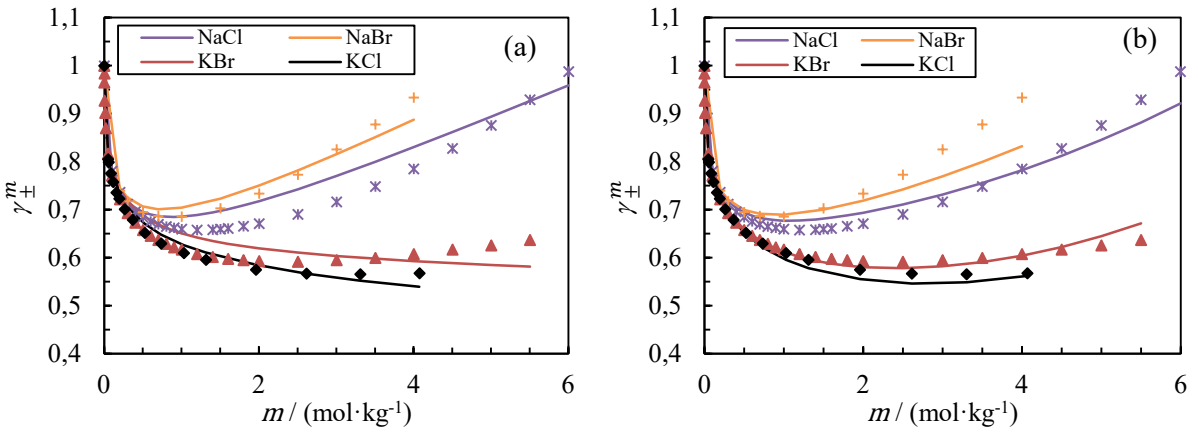

Figure 13 : Comparison of the mean ionic activity coefficient calculation for NaBr, NaCl, KBr and KCl salts at 298 K. (a) using model 1.0 and (b) using model 2.0. The symbols are the experimental data and the curves represent the model. Calculations were made at 1 bar.

As can be seen in Figure 13, both models follow the trend of the experimental data. Model 2.0 generates better results, especially for KBr and KCl salts.

The trend of the hard sphere ionic parameters is shown in Figure 14. The MSA diameters are systematically obtained by multiplying the hard sphere diameter by 1.5 (see equation (54)). It appears that for the model 2.0, the fitted parameters are very close to those of Pauling, except for the diameter of the ion Br^- which is smaller than the Pauling diameter. For model 1.0, a small inversion is observed, the diameter of the potassium is larger than the diameter of the chlorine.

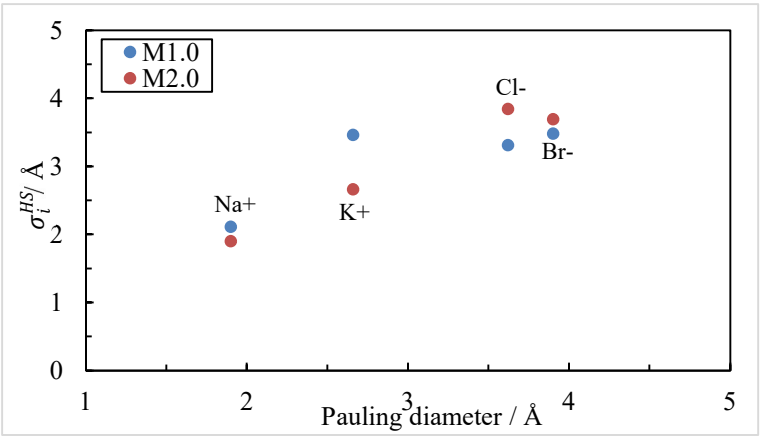

Figure 14 : Comparison of the hard sphere diameters obtained for the models 1.0 (M1.0) and 2.0 (M2.0), with the Pauling diameter. Blue points are dispersive model 1.0 and red points are associative model 2.0.

5.1.3 Regarding the maximum of mean ionic activity coefficient with temperature

As shown by Vaque Aura et al. [29] the dependence of the mean ionic activity coefficient with temperature for the 4 salts considered presents an increase and in some cases a maximum, as can be seen

in Figure 15. As mentioned above, this type of behaviour is difficult to capture, even for NaCl, where the enthalpy of solution values that are included in the objective function reach large molalities (up to 5 molal as shown for example in Figure 12(b)). For all other salts, the deviations on the enthalpy of solution are very small because the data are insignificant (concentration below 0.6 molal), and as a consequence, the mean ionic activity coefficient continually decreases with temperature.

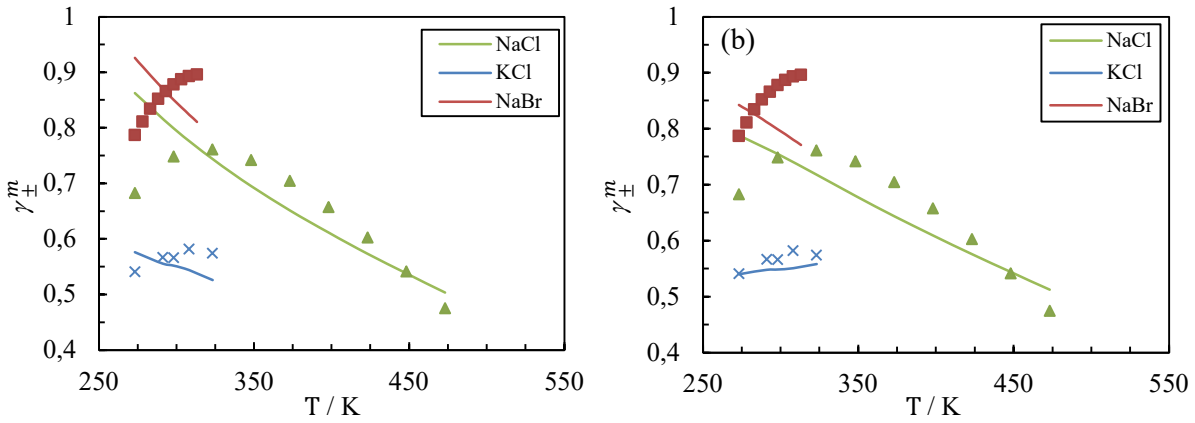

Figure 15 : Variation of mean ionic activity coefficient with respect to temperature at 3.5 molal. The dots represent the experimental data and the curves the model. (a) Model 1.0 and (b) Model 2.0.

A possible way to correct the model is to include temperature-dependent interaction parameters. Using model 1, this has been done in the past [89]. For model 2.0, the framework of the association term leads to a decrease of association force when temperature increases. It is not designed to allow for changing this dependence.

5.2 Representation of the Gibbs energy of solvation

Even though the Born radius is calculated from the Gibbs energy of solvation, it is be worth assessing if this property can be described accurately. Using the SAFT framework, the Gibbs energy of solvation of an ion is directly related to the fugacity coefficient of that ion at infinite dilution in water:

$$\frac{\Delta_s G_i}{RT} = ln(\varphi_i^{\infty}) = \frac{1}{RT}\left(\sum \frac{\partial A^{\infty}}{\partial n_{ion}}\right) - ln\left(\frac{Z}{Z^{\infty}}\right) \tag{55}$$

In Table 19 the experimental values of the Gibbs energy of solvation and the calculated values for all the ions used in this work are shown. The calculated values were obtained using the parameters presented in Table 18. The AARD (%) of the calculated values does not exceed 5% with either model 1.0 or model 2.0.

Table 19 : Comparison between the experimental and calculated Gibbs energy of solvation for Na+, K+, Cl- and Br- ions, using dispersive and associative models [a]. $\Delta_s G_i Exp.$ is the experimental Gibbs energy of solvation and $\Delta_s G_i$ Calc is the Gibbs energy of solvation calculated with each model.

Cation	$\Delta_s G_i$ Exp. / kJ/mol [58]	$\Delta_s G_i$ Calc. / kJ/mol M1.0	$\Delta_s G_i$Calc. / kJ/mol M2.0	Anion	$\Delta_s G_i$Exp. / kJ/mol [58]	$\Delta_s G_i$Calc. / kJ/mol M1.0	$\Delta_s G_i$Calc. / kJ/mol M2.0
Na^+	-424.00	-429.44	-423.75	Cl^-	-304.00	-308.29	-313.69
K^+	-352.00	-358.16	-360.85	Br^-	-278.00	-281.88	-289.33

[a] The calculation of the Gibbs energy of solvation was done using the parameters presented in Table 18. M1.0 refers to the dispersive model 1.0 and M2.0 refers to the associative model 2.0.

5.3 Single ionic activity coefficients (SIAC)

A number of authors [27, 28], have tried to obtain data for the individual activity coefficient of the ions. For the NaCl salt, their results show that the activity coefficient of the cation is higher than the activity coefficient of the anion. This may indicate that the cation is more solvated than the anion. To compare

models 1.0 and 2.0 with these results, the individual activity coefficient for NaCl was calculated using the parameters presented in Table 18.

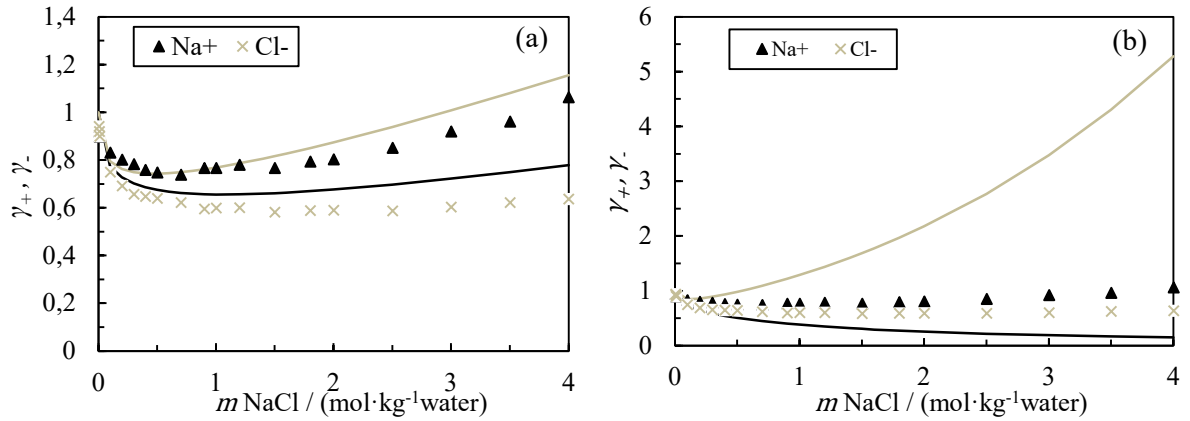

Figure 16 Individual activity coefficient (γ_+, γ_-) of chloride and sodium as a function of salt concentration at 298.15 K. (a) using model 1.0, (b) using model 2.0. The dots represent the experimental data [28] and curves the model. Calculations were made at 1 bar.

In Figure 16(a) model 1.0 shows an inverse behavior compared to the experimental data. Although the parameters appear to be physically consistent, the model is not able to reproduce this property correctly. This may be because the two dispersion energies are equal. In Figure 16(b) the trend is also inverse. This behaviour may be due to the very high value of the association energy of the anion (chlorine). For model 2.0 the association energy of the cation (sodium) was used as an adjustable parameter. Therefore, it may be assumed that this parameter compensates for the excess solvation of the anion, by decreasing the association energy of the cation. This would explain why the association energies of both ions in model 2.0 show an inverse behaviour to the expected one.

5.4 Comments on the contribution to the natural logarithm of mean ionic activity coefficient

Extracting conclusions by analysing the contribution of each term to the natural logarithm of the MIAC is quite complex. However, some observations have been made by comparing the contribution of terms for dispersive and associative models. In Figure 17 the two models that have been selected as the most accurate ones (in strategy "a") are compared (the corresponding plots for all models are available in supplementary information B).

In Figure 17(a) the dispersive approach is considered. In this case, both the dispersion and MSA terms generate a negative contribution. They are counterbalanced by the hard sphere, Born and association terms (water-water associations exist in this model, and they have an impact on the ionic activity coefficients). In contrast, the contributions using the association model, shown in Figure 17(b), the hard sphere term has a negative effect, in addition to MSA, and the association, much larger in magnitude, is the only significant positive contribution. The large, and opposite, contributions of the Hard Sphere term need to be further understood, but explain why the ionic hard sphere diameters have a large impact on the result.

The same trends are observed for all sub-models (i.e., using various types of dielectric constant functionalities). The Born contribution is obviously larger when using the Pottel correction, because the dielectric constant decreases much faster, but it does not change the global picture.

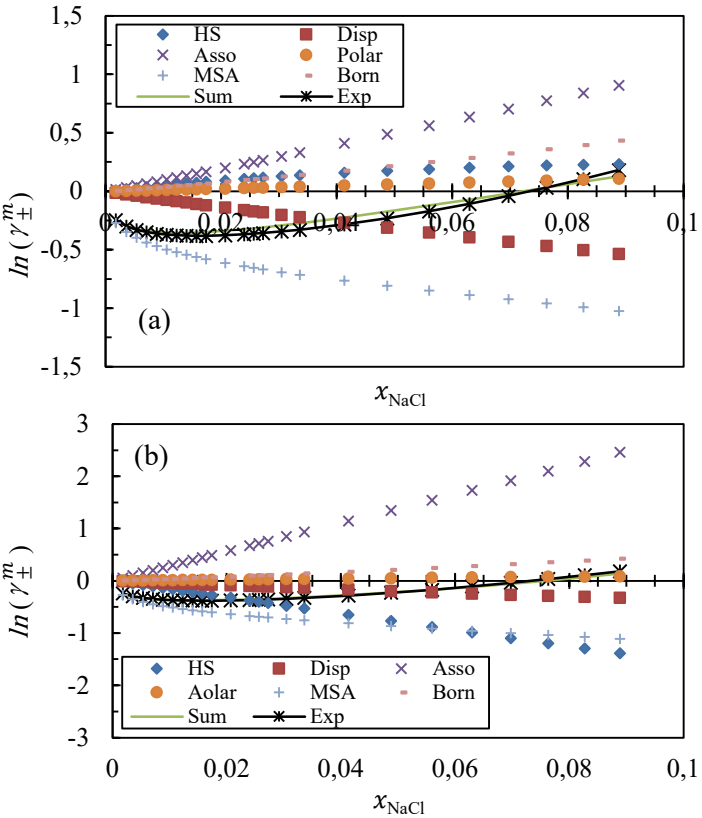

Figure 17 : Effect of the various terms on the natural logarithm of mean ionic activity coefficient for aqueous NaCl as a function of salt concentration at 298 K (a) using model 1.2 and (b) using model 2.0. Where HS=hard sphere, Disp=dispersion, Asso=association, Polar=polar, MSA= MSA and Born=Born terms, Sum = sum of all terms and Exp= experimental mean ionic activity coefficient data.

Conclusion

The objective of this work was to benchmark various PPC-SAFT-based equations of state for describing the temperature trend of mean ionic activity coefficient, and more particularly at the low temperature, where an anomalous behaviour is observed.

To this end, four important properties for NaCl aqueous solutions have been used (mean ionic activity coefficient, osmotic coefficient, enthalpy of solution and apparent molar volume). Three other salts (KBr, KCl, NaBr) have been investigated as extensions in the discussion section.

The use of enthalpy of solution data that cover a large concentration range and a low temperature range (below 323 K) is found to be consistent with a rising value of mean ionic activity coefficient at fixed molality in this low temperature range, resulting effectively in a maximum in the temperature trend close to 320 K. This trend has rarely been pointed out, and it appears that, to the best of our knowledge, no author has attempted to describe it. Our attempts to do so show that it is very difficult to model it for a model with physically consistent parameters. We believe that the only way to reach this goal would be to use temperature-dependent parameters.

Two modelling approaches have been compared. The main difference between the models is the way in which short-range interactions involving ions are considered (solvation interactions and ion pair formation), in addition to the different models used to describe the dielectric constant. The first approach (dispersive models) consists in using a dispersion term, while the second approach (associative models) consists in using the Wertheim association term. In both approaches the MSA term was used to account for long-range electrostatic interactions and the Born term to model electrostatic interactions between ions and solvent. No major difference in the capacity of modelling the target properties was found.

Three different sub-models have been used to calculate the dielectric constant of the solutions. In the present study it is observed that the addition of an explicit salt concentration dependence on top of the implicit Schreckenberg model [13] is not needed for the description of the activity coefficient for the system NaCl + water. The parameters that take into account the salt concentration ($\alpha_{0,ion}$ and $\alpha_{T,ion}$) for the Simonin correction tend to zero. Furthermore, a sensitivity analysis showed that these Simonin parameters have low influence on the objective function. In most cases, the models in which the Pottel dielectric constant was used gave the worst results. These results may indicate that it is not necessary to use an explicit salt concentration-dependent dielectric constant for the study of electrolytic systems. However, A more detailed study may help further clarifying these observations.

The use of the Born term remains essential, though, for representing Gibbs energies of solvation. For this property, the Born term has the largest impact, as was also shown by Fawcett [58].

This study has also identified the most sensitive parameters in modelling electrolyte solutions with PPC-SAFT, allowing a reduction of the number of adjustable parameters without significantly affecting the quality of the model. Some consistency constraints were also applied to obtain adequate results with physically consistent parameters. For the dispersive model, the hard sphere diameter (σ_i^{HS}) of both ions and the cation-anion dispersion energy ($\varepsilon_{\mathrm{Cat-}Ani}$) were identified as the most influential parameters. For associative model, the most influential parameters were the cation-water association energy ($\varepsilon_{Cat-Water}^{AB}$), the cation-anion association energy ($\varepsilon_{Cat-ani}^{AB}$) and the hard sphere diameter of the anion (σ_{anion}^{HS}). In both cases the parameters that consider the interactions between the cation and anion, were found to be quite influential in the model.

Acknowledgments

The authors acknowledge the financial support of the Chair EleTher IFP-School.

6 References

1 Li Z.-G., Sun Y.-Q., Zheng W.-L., Teng H., Xiu Z.-L. (2013) A novel and environment-friendly bioprocess of 1,3-propanediol fermentation integrated with aqueous two-phase extraction by ethanol/sodium carbonate system, *Biochemical Engineering Journal* **80**, 68–75. DOI: 10.1016/j.bej.2013.09.014.

2 Roa Pinto J.S., Bachaud P., Fargetton T., Ferrando N., Jeannin L., Louvet F. (2021) Modeling phase equilibrium of hydrogen and natural gas in brines: Application to storage in salt caverns, *International Journal of Hydrogen Energy* **46**, 5, 4229–4240. DOI: 10.1016/j.ijhydene.2020.10.242.

3 Jouyban A. (2010) *Handbook of Solubility Data for Pharmaceuticals*, CRC Press, United States of America.

4 Gang Jin and Marc D. Donohue (1991) An equation of state for electrolyte solutions.: 3. Aqueous solutions containing multiple salts, *American Chemical Society* **30**, 1, 240–248.

5 Pinsky M.L., Takano K. (2004) Chater 8: Property Estimation for Electrolyte Systems, in *Computer Aided Property Estimation for Process and Product Design*, Elsevier, pp. 181–204.

6 Maribo-Mogensen B. (2014) Development of an Electrolyte CPA Equation of state for Applications in the Petroleum and Chemical Industries, *PhD*, Technical University of Denmark.

7 Kontogeorgis G.M., Maribo-Mogensen B., Thomsen K. (2018) The Debye-Hückel theory and its importance in modeling electrolyte solutions, *Fluid Phase Equilibria* **462**, 130–152. DOI: 10.1016/j.fluid.2018.01.004.

8 Ahmed S. (2019) Thermodynamic modeling of mixed-solvent electrolytes for process simulators, *Thèse de doctorat*, Sorbonne Université.

9 Ahmed S., Ferrando N., Hemptinne J.-C. de, Simonin J.-P., Bernard O., Baudouin O. (2018) Modeling of mixed-solvent electrolyte systems, *Fluid Phase Equilibria* **459**, 138–157. DOI: 10.1016/j.fluid.2017.12.002.

10 Maribo-Mogensen B., Kontogeorgis G.M., Thomsen K. (2012) Comparison of the Debye–Hückel and the Mean Spherical Approximation Theories for Electrolyte Solutions, *Ind. Eng. Chem. Res.* **51**, 14, 5353–5363. DOI: 10.1021/ie2029943.

11 Rozmus J., Hemptinne J.-C. de, Galindo A., Dufal S., Mougin P. (2013) Modeling of Strong Electrolytes with ePPC-SAFT up to High Temperatures, *Ind. Eng. Chem. Res.* **52**, 29, 9979–9994. DOI: 10.1021/ie303527j.

12 Herzog S., Gross J., Arlt W. (2010) Equation of state for aqueous electrolyte systems based on the semirestricted non-primitive mean spherical approximation, *Fluid Phase Equilibria* **297**, 1, 23–33. DOI: 10.1016/j.fluid.2010.05.024.

13 Schreckenberg J.M., Dufal S., Haslam A.J., Adjiman C.S., Jackson G., Galindo A. (2014) Modelling of the thermodynamic and solvation properties of electrolyte solutions with the statistical associating fluid theory for potentials of variable range, *Molecular Physics* **112**, 17, 2339–2364. DOI: 10.1080/00268976.2014.910316.

14 Eriksen D.K., Lazarou G., Galindo A., Jackson G., Adjiman C.S., Haslam A.J. (2016) Development of intermolecular potential models for electrolyte solutions using an electrolyte SAFT-VR Mie equation of state, *Molecular Physics* **114**, 18, 2724–2749. DOI: 10.1080/00268976.2016.1236221.

15 Simonin J.-P. (2019) On the "Born" term used in thermodynamic models for electrolytes, *The Journal of Chemical Physics* **150**, 24, 244503. DOI: 10.1063/1.5096598.

16 Karl Giese/U. Kaatze/R. Pottel (1970) Permittivity and dielectric and proton magnetic relaxation of aqueous solutions of the alkali halides, *The Journal of Physical Chemistry,* **74**, 21.

17 Simonin J.-P., Bernard O., Blum L. (1998) Real Ionic Solutions in the Mean Spherical Approximation. 3. Osmotic and Activity Coefficients for Associating Electrolytes in the Primitive Model, *Journal of physics chemical*, 102, 4411–4417.

18 Held C. (2020) Thermodynamic gE Models and Equations of State for Electrolytes in a Water-Poor Medium: A Review, *J. Chem. Eng. Data* **65**, 2073–5082.

19 Simonin J.-P., Bernard O., Blum L. (1999) Ionic Solutions in the Binding Mean Spherical Approximation: Thermodynamic Properties of Mixtures of Associating Electrolytes, *J. Phys. Chem. B* **103**, 4, 699–704. DOI: 10.1021/jp9833000.

20 Galindo A., Gil-Villegas A., Jackson G., Burgess A.N. (1999) SAFT-VRE: Phase Behavior of Electrolyte Solutions with the Statistical Associating Fluid Theory for Potentials of Variable Range, *J. Phys. Chem. B* **103**, 46, 10272–10281. DOI: 10.1021/jp991959f.

21 Mark Bulow, Moreno Ascani, Christoph Held (2021) ePC-SAFT advanced - Part I: Physical meaning of including a concentration-dependent dielectric constant in the born term and in the Debye-Hückel theory, *Fluid Phase Equilibria* **535**, 1–8.

22 Mark Bulow, Moreno Ascani, Christoph Held (2021) ePC-SAFT advanced - Part II: Application to Salt Solubility in Ionic and Organic Solvents and the Impact of Ion Pairing, *Fluid Phase Equilibria* **537**, 1–11.

23 Prausnitz, J. M., Lichtenthaler, R. N., & De Azevedo, E. G (1998) *Molecular thermodynamics of fluid-phase equilibria*, Pearson Education.

24 Schlaikjer A., Thomsen K., Kontogeorgis G.M. (2017) Simultaneous Description of Activity Coefficients and Solubility with eCPA, *Ind. Eng. Chem. Res.* **56**, 4, 1074–1089. DOI: 10.1021/acs.iecr.6b03333.

25 Hemptinne J.-C. de, Ledanois J.-M., Mougin P., Barreau A. (2012) *Select thermodynamic models for process simulation: A practical guide using a three steps methodology*, Editions Technip, Paris. ISBN: 9782710809494.

26 Thomsen K. (2009) Electrolyte Solutions: Thermodynamics, Crystallization, Separation Methods, *DTU Library* **1**, 1–111.

27 Rodil E., Vera J.H. (2001) Individual activity coefficients of chloride ions in aqueous solutions of MgCl2, CaCl2 and BaCl2 at 298.2 K, *Fluid Phase Equilibria* **15–27**, 187–188, 15–27.

28 Wilczek-Vera G., Rodil E., Vera J.H. (2004) On the activity of ions and the junction potential: Revised values for all data, *AIChE Journal* **50**, 2, 445–462.

29 Vaque Aura S., Roa Pinto J.-S., Ferrando N., Hemptinne J.-C. de, Kate A. ten, Kuitunen S., Diamantonis N., Gerlach T., Heilig M., Becker G., Brehelin M. (2021) Data Analysis for Electrolyte Systems: A Method Illustrated on Alkali Halides in Water, *J. Chem. Eng. Data* **66**, 8, 2976–2990. DOI: 10.1021/acs.jced.1c00105.

30 Bockris, J. O. M., Reddy, A. K., & Gamboa-Aldeco, M. E. (1998) *Modern electrochemistry: electrodics in chemistry, engineering, biology and environmental science*, Springer Science & Business Media.

31 H. Frank Gibbard Jr., George Scatchard, Raymond A. Rousseau, and Jefferson L. Creek Liquid-vapor equilibrium of aqueous sodium chloride, from 298 to 373.deg.K and from 1 to 6 mol kg-1, and related properties.

32 Harned H.S., Nims L.F. (1932) The thermodynamic properties of aqueous sodium chloride solutions from 0 to 40°, *Journal of the American Chemical Society* **54**, 2, 423–432.

33 Smith W.R., Moučka F., Nezbeda I. (2016) Osmotic pressure of aqueous electrolyte solutions via molecular simulations of chemical potentials: Application to NaCl, *Fluid Phase Equilibria* **407**, 76–83. DOI: 10.1016/j.fluid.2015.05.012.

34 Bousfield W.R., Bousfield C.E. (1918) Vapour pressure and density of sodium chloride solutions, *Trans. Faraday Soc.* **13**, 401.

35 Vaslow F. (1966) The Apparent Molal Volumes of the Alkali Metal Chlorides in Aqueous Solution and Evidence for Salt-Induced Structure Transitions, *Journal of Physical Chemistry* **710**, 7, 2286–2294.

36 Zarembo V.I., Fedorov M. (1975) Density of sodium chloride solutions in the 25 - 350 degrees range and pressure up to 1000 kg-force/cm2., *Zh. Prikl. Khim.* **48**, 1949–1953.

37 Robinson R.A., Stokes R.H. (2002) *Electrolyte solutions*, Courier Corporation.

38 Taniewska-Osinska S., Logwinienko R. (1976) Calorimetric Investigations of Aqueous Solutions of Sodium Chloride and Cobalt(II) Chloride at Several Temperatures., *Acta Univ. Lodz. Ser* **2**, 69–75.

39 Lu Y., Zhen S., Lu J. (1992) The enthalpic interaction parameters of NaCl, KCl and KI with acetone in water at 298.15 K, *Thermochim. Acta* **210**, 15–25.

40 Sanahuja A. (1985) Enthalpy of Solution of KCl in Water at 308.15 and 313.15 K, *J. Chem. Thermodyn.* **17**, 1063–1066.

41 Wallace W.E. (1949) Heats of Dilution of Aqueous Sodium Bromide and the Standard Heat of Solution of Sodium Bromide at 25°, *J. Am. Chem. Soc.* **71**, 2485–2487.

42 Woldan M. (1987) Enthalpies of Transfer of Alkali Metal Halides from Water to Water - Acetamide Mixtures, *Thermochim. Acta* **111**, 175–183.

43 Semin A.V., Klopov V.I. (1979) Thermochemistry of Potassium Bromide Dissolution in Mixtures of Water with tert-Butanol at 10 - 40 °C, *Izv. Vyssh. Uchebn. Zaved. Khim. Khim. Tekhnol.* **22**, 2, 248–250.

44 Rozmus J., Brunella I., Mougin P., Hemptinne J.-C. de (2012) Isobaric Vapor–Liquid Equilibria of Tertiary Amine and n -Alkane/Alkanol Binary Mixtures: Experimental Measurements and Modeling with GC-PPC-SAFT, *J. Chem. Eng. Data* **57**, 11, 2915–2922. DOI: 10.1021/je300568h.

45 Debye P., Hückel E. (1923) Zur Theorie der Elektrolyte: I: Gefrierpunktserniedrigung und verwandte Erscheinungen., *Phys. Z.* **24**, 185–207.

46 Wei D., Blum L. (1987) The mean spherical approximation for an arbitrary mixture of ions in a dipolar solvent: Approximate solution, pair correlation functions, and thermodynamics, *The Journal of Chemical Physics* **87**, 5, 2999–3007. DOI: 10.1063/1.453036.

47 Von M. Born (1920) Volumen und Hydratationswärme der Ionen, *Phys. Ges.* **21**, 13, 45–48.

48 Ahmed S., Ferrando N., Hemptinne J.-C. de, Simonin J.-P., Bernard O., Baudouin O. (2016) A New PC-SAFT Model for Pure Water, Water–Hydrocarbons, and Water–Oxygenates Systems and Subsequent Modeling of VLE, VLLE, and LLE, *J. Chem. Eng. Data* **61**, 12, 4178–4190. DOI: 10.1021/acs.jced.6b00565.

49 Carnahan N.F., Starling K.E. (1972) Intermolecular repulsions and the equation of state for fluids, *AIChE J.* **18**, 6, 1184–1189.

50 Mansoori G.A., Carnahan N.F., Starling K.E., Leland T.W. (1971) Equilibrium Thermodynamic Properties of the Mixture of Hard Spheres, *The Journal of Chemical Physics* **54**, 4, 1523–1525. DOI: 10.1063/1.1675048.

51 Gross J., Sadowski G. (2001) Perturbed-Chain SAFT: An Equation of State Based on a Perturbation Theory for Chain Molecules, *Ind. Eng. Chem. Res.* **40**, 4, 1244–1260. DOI: 10.1021/ie0003887.

52 Boublik T. (2006) Perturbation theory of pure quadrupolar hard gaussian overlap fluids, *Molecular Physics* **69**, 3, 497–505. DOI: 10.1080/00268979000100361.

53 Chapman W.G., Jackson G., Gubbins K.E. (1988) Phase equilibria of associating fluids: Chain molecules with multiple bonding sites, *Molecular Physics* **65**, 5, 1057–1079. DOI: 10.1080/00268978800101601.

54 NguyenHuynh D., Passarello J.-P., Tobaly P., Hemptinne J.-C. de (2008) Application of GC-SAFT EOS to polar systems using a segment approach, *Fluid Phase Equilibria* **264**, 1-2, 62–75. DOI: 10.1016/j.fluid.2007.10.019.

55 NguyenHuynh D., Passarello J.-P., Hemptinne J.-C. de, Tobaly P. (2011) Extension of polar GC-SAFT to systems containing some oxygenated compounds: Application to ethers, aldehydes and ketones, *Fluid Phase Equilibria* **307**, 2, 142–159. DOI: 10.1016/j.fluid.2011.04.009.

56 Jog P.K., Sauer S.G., Blaesing J., Chapman W. G. (2001) Application of Dipolar Chain Theory to the Phase Behavior of Polar Fluids and Mixtures, *Ind. Eng. Chem. Res.*, 40, 4641–4648.

57 Maribo-Mogensen B., Thomsen K., Kontogeorgis G.M. (2015) An electrolyte CPA equation of state for mixed solvent electrolytes, *AIChE J.* **61**, 9, 2933–2950. DOI: 10.1002/aic.14829.

58 Fawcett W.R. (1999) Thermodynamic Parameters for the Solvation of Monatomic Ions in Water, *J. Phys. Chem. B* **103**, 50, 11181–11185. DOI: 10.1021/jp991802n.

59 Myers J.A., Sandler S.I., Wood R.H. (2002) An Equation of State for Electrolyte Solutions Covering Wide Ranges of Temperature, Pressure, and Composition, *Ind. Eng. Chem. Res.* **41**, 13, 3282–3297. DOI: 10.1021/ie011016g.

60 Inchekel R., Hemptinne J.-C. de, Fürst W. (2008) The simultaneous representation of dielectric constant, volume and activity coefficients using an electrolyte equation of state, *Fluid Phase Equilibria* **271**, 1-2, 19–27. DOI: 10.1016/j.fluid.2008.06.013.

61 Kontogeorgis G.M., Folas G.K. (2009) *Thermodynamic Models for Industrial Applications: From Classical and Advanced Mixing Rules to Association Theories*, John Wiley & Sons.

62 Rozmus J. (2012) Équation d'état électrolyte prédictive pour le captage du CO2 Predictive electrolyte equation of state for CO2 capture, *PhD*, UNIVERSITE PIERRE ET MARIE CURIE.

63 Maribo-Mogensen B., Kontogeorgis G.M., Thomsen K. (2013) Modeling of dielectric properties of aqueous salt solutions with an equation of state, *The journal of physical chemistry. B* **117**, 36, 10523–10533. DOI: 10.1021/jp403375t.

64 Maribo-Mogensen B., Kontogeorgis G.M., Thomsen K. (2013) Modeling of dielectric properties of complex fluids with an equation of state, *The journal of physical chemistry. B* **117**, 12, 3389–3397. DOI: 10.1021/jp310572q.

65 Chia-tsun L.2., W. T. Lindsay JR. (1972) Thermodynamics of sodium chloride solutions at high temperatures, *Journal of Solution Chemistry* **1**, 1, 45–69.

66 Rodney P. Smith/Donald S. Hirtle (1939) The Boiling Point Elevation. III. Sodium Chloride 1.0 to 4.0 <italic>M</italic> and 60 to 100°, *Department of Chemistry of Yale University* **61**, 1123–1126.

67 Hamer W.J., Wu Y.C. (1972) Osmotic Coefficients and Mean Activity Coefficients of Uni-Univalent Electrolytes in Water at 25 °C, *J. Phys. Chem. Ref. Data* **1**, 4, 1047–1099.

68 Gèrald Perron, Alain Roux, and Jacques E. Desnoyers (1981) Heat capacities and volumes of NaCl, MgCl2, CaCl2, and NiCl2 up to 6 molal in water, *CAN J. CHEM.* **59**, 3049–3054.

69 Pauling L. (1960) *The Nature of the Chemical Bond*, Cornell University Press.

70 R. D. SHANNON (1976) Revised effective ionic radii and systematic studies of interatomic distances in halides and chalcogenides, *Acta Cryst.* **32**, 751–767.

71 Trinh T.-K.-H., Passarello J.-P., Hemptinne J.-C. de, Lugo R., Lachet V. (2016) A non-additive repulsive contribution in an equation of state: The development for homonuclear square well chains equation of state validated against Monte Carlo simulation, *The Journal of Chemical Physics* **144**, 12, 124902. DOI: 10.1063/1.4944068.

72 Held C., Cameretti L.F., Sadowski G. (2008) Modeling aqueous electrolyte solutions: Part 1. Fully dissociated electrolytes, *Fluid Phase Equilibria* **270**, 1-2, 87–96. DOI: 10.1016/j.fluid.2008.06.010.

73 Held C., Sadowski G. (2009) Modeling aqueous electrolyte solutions. Part 2. Weak electrolytes, *Fluid Phase Equilibria* **279**, 2, 141–148. DOI: 10.1016/j.fluid.2009.02.015.

74 Delphine S. (2017) *Advanced Tools for Optimization and Uncertainty Treatment: USER MANUAL*, IFPEN, Paris France.

75 Caramazza R. (1960) Measurement of the activity coefficients of potassium chloride in aqueous solution, *Gazz. Chim. Ital.* **90**, 1721–1729.

76 Hernández-Luis F., Rodríguez-Raposo R., Galleguillos H.R., Morales J.W. (2010) Activity coefficients of KCl in PEG 4000+water mixtures at 288.15, 298.15 and 308.15K, *Fluid Phase Equilibria* **295**, 2, 163–171. DOI: 10.1016/j.fluid.2010.04.012.

77 R. H. Stokes/Barbara J. Levien (1946) The Osmotic and Activity Coefficients of Zinc Nitrate, Zinc Perchlorate and Magnesium Perchlorate. Transference Numbers in Zinc Perchlorate Solutions, *J. Am. Chem. Soc.* **68**, 2, 333–337.

78 Platford R.F. (1973) Osmotic coefficients of aqueous solutions of seven compounds at 0.deg., *J. Chem. Eng. Data* **18**, 2, 215–217.

79 Thomas M. Davis/Lisa M. Duckett/Judith F. Owen/C. Stuart Patterson/Robert Saleeby (1985) Osmotic coefficients of aqueous lithium chloride and potassium chloride from their isopiestic ratios to sodium chloride at 45.degree.C, *J. Chem. Eng. Data* **30**, 4, 432–434.

80 John T. Moore/William T. Humphries/C. Stuart Patterson (1972) Isopiestic studies of some aqueous electrolyte solutions at 80.deg., *J. Chem. Eng. Data* **17**, 2, 180–182.

81 Patterson C.S., Gilpatrick L.O., Soldano B.A. (1960) The Osmotic Behaviour of Representative Aqueous Salt Solutions at 100°C, *J. Chem. Soc.* **37**, 2730–2734.

82 Soldano B.A., Meek M. (1963) Isopiestic Vapour-Pressure Measurements of Aqueous Salt Solutions at Elevated Temperatures. Part III., *J. Chem. Soc.* **1**, 4424–4426.

83 Herbert S. Harned/Chester C. Crawford (1937) The Thermodynamics of Aqueous Sodium Bromide Solutions from Electromotive Force Measurements[1], *J. Chem. Eng. Data* **1**, 1903–1905.

84 Christov C. (2007) An isopiestic study of aqueous NaBr and KBr at 50°C: Chemical equilibrium model of solution behavior and solubility in the NaBr–H2O, KBr–H2O and Na–K–Br–H2O systems to high concentration and temperature, *Geochimica et Cosmochimica Acta* **71**, 14, 3557–3569. DOI: 10.1016/j.gca.2007.05.007.

85 Voigt W., Dittrich A., Haugsdal B., Grjotheim K. (1990) Thermodynamics of Aqueous Reciprocal Salt Systems. II. Isopiestic Determination of the Osmotic and Activity Coefficients in LiNO3 - NaBr - H2O and LiBr - NaNO3 - H2O at 100. °C, *Acta Chem. Scand.* **44**, 12–17.

86 Holmes, H. F. and Mesmer, R. E. (1998) An isopiestic study of aqueous solutions of the alkali metal bromides at elevated temperatures, *J. Chem. Thermodyn.* **30**, 723–741.

87 George C. Johnson/Rodney P. Smith (1941) The Boiling Point Elevation. IV. Potassium Bromide in Water[1], *J. Am. Chem. Soc.* **63**, 1351–1353.

88 Gorbachev S.V., Kondratev V.P., Androsov V.I. (1974) Specific volumes of potassium bromide, iodide, and nitrate solutions in water., *Zh. Fiz. Khim.* **48**, 11, 2675–2677.

89 Pabsch D., Held C., Sadowski G. (2020) Modeling the CO 2 Solubility in Aqueous Electrolyte Solutions Using ePC-SAFT, *J. Chem. Eng. Data* **65**, 12, 5768–5777. DOI: 10.1021/acs.jced.0c00704.